PHYSICAL REVIEW D **89,** 014017 (2014)

Implication of nonuniversal Z' boson to the lepton polarization asymmetries in the $B \to K^* \ell^+ \ell^-$ decay

Ishtiaq Ahmed[*]

National Centre for Physics, Quaid-i-Azam University Campus, Islamabad 45320, Pakistan

(Received 26 September 2013; published 21 January 2014)

In this work we study the implication of the nonuniversal Z' model to the double lepton polarization asymmetries in the $B \to K^* \ell^+ \ell^-$, $(l = \mu, \tau)$ decay. To see the variation in the values of lepton polarization asymmetries from the standard model values, we have taken bounds of the UTfit collaboration, namely, S_1 and S_2 on the values of different parameters of the universal Z' model such as left-right couplings of the extra gauge boson with leptons and the new weak phase ϕ_{sb}. It is found that double lepton polarization asymmetries are sensitive to the coupling parameters of Z' boson with fermions. Therefore, the measurements of these lepton polarization asymmetries for the above-mentioned decay at current colliders can be helpful to clarify the status of the existence of the extra gauge boson, i.e., Z'.

DOI: 10.1103/PhysRevD.89.014017 PACS numbers: 14.40.Nd, 13.20.He, 12.60.-i

I. INTRODUCTION

The understanding of flavor dynamics is one of the most important goals of elementary particle physics because this understanding gives us more insight about short distance scales phenomena. In this regard, the standard model (SM) of particle physics has been very successful. It describes three fundamental interactions out of four with great accuracy. The standard model encodes the myriad of particle interactions in terms of a simple Lagrangian wherein quarks and gluons interact highly nonlinearly via what is called quantum chromodynamics while quarks and leptons interact with heavy gauge bosons Z, W in a unified picture of the weak and electromagnetic interaction based on the symmetry $SU(2)_L \times U_y(1)$. This simple and elegant picture has been subject to numerous experimental probes at a range of energies from threshold to nearly the TeV level and has passed each test successfully.

Nevertheless, there exist some strong fundamental reasons to suspect that there is something beyond the standard model. Apart from these fundamental shortcomings there are some discrepancies between the experimental data and the predictions of the SM that have been observed in the last few years [1–5]. To address the above-mentioned shortcomings and to overcome the experimental discrepancies many models have been proposed such as the little Higgs model [6,7], Extra dimensions model like the Applequest-Cheng-Dobrescu model [8], the minimal super symmetric SM [9], nonuniversal Z' model [10], and the SM with 4th generation [11]. Among these the Z' model seems to be a simple and straightforward extension of the gauge group $SU(2)_L \times U(1)$. Besides its simplicity this model has a potential to solve some problems which occur in the SM [12–14]. Moreover, it has a new weak phase which may enhance charge parity violation and can provide a natural way to accommodate the excess in CP violation measurements which have been observed in some B—meson decays [15–20].

On the other hand, the key area of contemporary particle physics deals with searches for so-called BSM (beyond standard model) physics. Since no such definitive signal has yet been observed, it is impossible to say exactly what form such a BSM interaction might take. Nevertheless, it is important to identify possible mechanisms whereby this might happen and to locate experimental signals that could be optimal for a BSM observation. Regarding this, flavor changing neutral currents (FCNC) provide a fertile ground to test the SM at loop level as well as probe to BSM physics. As we have mentioned earlier, the standard model has so far passed all experimental tests at the highest energy accelerator available today, namely the LHC at CERN. It is clear that BSM pictures must involve particles which are much heavier than those presently accessible, and therefore it is a challenge to see how to probe for the existence of such structures. In this context, FCNC may be used as a probe of BSM physics since the Z-boson couples only to quarks/leptons with the same flavor; therefore, FCNC effects do not arise at tree level and must occur through loops. Of course, this effect already occurs in the standard model, with the usual particles present in the loops. However, BSM particles will lead to additional contributions to the FCNC process where the contribution of such BSM effects might be optimal for experimental detection. In this regard, $b \to s$ FCNC transition plays a crucial role in investigating the different new physics scenarios [21–29]. In the same way, the Z' boson belonging to the new $U'(1)$ symmetry runs in the loop, consequently, only the Wilson coefficients get modified while the operator basis remains

[*]ishtiaq@ncp.edu.pk

the same as in the SM. As mentioned above a large number of complementary studies are needed because we do not know exactly the form of new physics. In this context, the semileptonic decay channels based on the $b \to s$ transitions provide a number of observables such as the forward-backward asymmetry (FBA), helicity fractions, single and double lepton polarization asymmetries, etc. The measurements of these observables at current colliders may provide useful information to sketch out the structure of proposed theories beyond the SM. Therefore, to explore the physics beyond the SM various inclusive B meson decays like $B \to X_{s,d}\ell^+\ell^-$ and their corresponding exclusive processes, like $B \to M\ell^+\ell^-$ with $M = K$, K^*, K_1, ρ etc have been investigated in the literature [30–47]. In these studies a large number of observables are examined which showed that the above mentioned inclusive and exclusive decays of B meson are very sensitive to the flavor structure of the standard model and receive corrections in many new physics (NP) models. Furthermore, among the various inclusive and exclusive semileptonic B meson decays, $B \to K^* l^+ l^-$ is of particular interest because it has a larger branching ratio that the other leptonic and semileptonic decay channels. With this motivation in this manuscript we have studied the effects of a family nonuniversal Z' model on the lepton polarization asymmetries in $B \to K^* l^+ l^-$ decays, where $l = \mu$ or τ.

This paper is organized as follows: In Sec. II we describe the theoretical formulation necessary to describe the $b \to s$ transition, including the effective Hamiltonian, matrix elements in terms of form factors, and the explicit form of the amplitude in terms of the matrix elements. In Sec. III we define the polarization asymmetries and write down the explicit expressions of these asymmetries for $B \to K^* l^+ l^-$. In Sec. IV we present the phenomenological analysis and discuss our numerical results. The last section is devoted to summarizing our work and to the conclusions.

II. THEORETICAL FORMULATION

The decay channel in which we are interested ($B \to K^* l^+ l^-$, $l = \mu$, τ) is the FCNC transition and originates from the quark level transition $b \to s l^+ l^-$. The QCD corrected effective Hamiltonian responsible for the $b \to s l^+ l^-$ transition can be written as follows

$$H_{\rm eff} = -\frac{4G_F}{\sqrt{2}} V_{tb}^* V_{ts} \sum_{i=1}^{10} C_i(\mu) O_i(\mu), \tag{1}$$

where $O_i(\mu)$ $(i = 1, \ldots, 10)$ are the four-quark operators and $C_i(\mu)$ are the corresponding Wilson coefficients at the energy scale μ and the explicit expressions of these coefficients in the SM at NLO and NNLL are given in [42,48–59]. Here, we have neglected the terms proportion to $V_{ub}V_{us}^*$ because of $\frac{V_{ub}V_{us}^*}{V_{tb}V_{ts}^*} < 0.02$. The operators responsible for $B \to K^*\ell^+\ell^-$ are O_7, O_9 and O_{10} are

$$\begin{aligned} O_7 &= \frac{e^2}{16\pi^2} m_b (\bar{s}\sigma_{\mu\nu} P_R b) F^{\mu\nu}, \\ O_9 &= \frac{e^2}{16\pi^2} (\bar{s}\gamma_\mu P_L b)(\bar{l}\gamma^\mu l), \\ O_{10} &= \frac{e^2}{16\pi^2} (\bar{s}\gamma_\mu P_L b)(\bar{l}\gamma^\mu\gamma_5 l), \end{aligned} \tag{2}$$

with $P_{L,R} = (1 \pm \gamma_5)/2$.

Neglecting the mass of the s-quark, the above effective Hamiltonian gives us the following matrix elements

$$\begin{aligned} &\mathcal{M}(B \to K^* l^+ l^-) \\ &= \Big[\frac{\alpha_{\rm em} G_F}{2\sqrt{2}\pi} V_{tb}^* V_{ts} \langle K^*(k,\varepsilon)|\bar{s}\gamma^\mu(1-\gamma^5)b|B(p)\rangle \\ &\quad \times \{C_9^{\rm eff}(\bar{l}\gamma^\mu l) + C_1 0(\bar{l}\gamma^\mu\gamma^5 l)\} \\ &\quad - 2C_7^{\rm eff} m_b \langle K^*(k,\varepsilon)|\bar{s} i\sigma_{\mu\nu}\frac{q^\nu}{s}(1+\gamma^5)b|B(p)\rangle(\bar{l}\gamma^\mu l)\Big], \end{aligned} \tag{3}$$

where q is the momentum transferred to the final lepton pair, i.e., $q = p_1 + p_2$ where p_1 and p_2 are the momenta of l^- and l^+, respectively, s is the squared of the momentum transfer, and $V_{tb}^* V_{ts}$ are the Cabibo-Kobayashi-Maskawa (CKM) matrix elements.

The Wilson coefficient $C_9^{\rm eff}$ contains a perturbative part which includes the indirect contributions of operators O_i where $i = 1$ to 6 and a nonperturbative or resonant part which contains the long-distance effects due to conversion of the real $c\bar{c}$ into the lepton pair $l^+ l^-$

$$C_9^{\rm eff} = C_9^{\rm per} + C_9^{\rm res}. \tag{4}$$

The perturbative part of $C_9^{\rm eff}$ reads [59]

$$\begin{aligned} C_9^{\rm per} &= C_9(m_b) + g(m_c, s)\left(\frac{4}{3}C_1 + C_2 + 6C_3 + 60C_5\right) \\ &\quad - \frac{2}{2}g(m_b, s)\left(7C_3 + \frac{4}{3}C_4 + 76C_5 + \frac{64}{3}C_6\right) \\ &\quad - \frac{1}{2}g(0, s)\left(C_3 + \frac{4}{3}C_4 + 16C_5 + \frac{64}{3}\right) \\ &\quad + \frac{4}{3}C_3 + \frac{64}{9}C_5 + \frac{64}{27}C_6, \end{aligned} \tag{5}$$

where the function $g(m_i, s)$ includes the one-loop correction to the four-quark operators $O_1, \ldots\ldots O_6$ and has the form [60,61]

$$g(m_i,s) = \frac{8}{27} - \frac{8}{9}\ln(m_i) + \frac{4}{9}y_i - \frac{2}{9}(2+y_i)\sqrt{|1-y_i|} \times \begin{cases} \left(\ln\left|\frac{\sqrt{1-y_i}+1}{\sqrt{1-y_i}-1}\right| - i\pi\right), & \text{for } y_i \le 1 \\ 2\arctan\frac{1}{\sqrt{y_i-1}}, & \text{for } y_i > 1, \end{cases} \quad (6)$$

where $y \equiv 4m_i^2/s$. $C_9^{\rm res}$ can be parametrized by using the Breit-Wigner formula in the following way

$$C_9^{\rm res} = -\frac{3\pi}{\alpha^2}\kappa[3C_1 + C_2 + 3C_3 + C_4 + 3C_5 + C_6]\sum_{V=\psi}\frac{m_V B_r(V\to l^+l^-)\Gamma^V_{\rm total}}{s - m_V^2 + im_V\Gamma_{{\rm total}^V}}. \quad (7)$$

As stated in the introduction, due to the presence of off-diagonal couplings in the Z' model, FCNC transitions can occur at the tree level. In this regard, to reduce the number of parameters, the Z-Z' mixing and the interaction of a right-handed quark with Z' are usually ignored [62]. Therefore, the Z' boson contribution modifies only the Wilson coefficients C_9 and C_{10}. With these assumptions, the additional part of the effective Hamiltonian due to the Z' contribution can be written as follows [63,47,64,65]

$$\mathcal{H}^{Z'}_{\rm eff} = -\frac{2G_F}{\sqrt{2}}\bar{s}\gamma^\mu(1-\gamma^5)b \times B_{sb}[-\mathcal{S}^L_{\ell\ell}\bar{\ell}\gamma^\mu(1-\gamma^5)\ell - \mathcal{S}^R_{\ell\ell}\bar{\ell}\gamma^\mu(1+\gamma^5)\ell] + \text{H.c}, \quad (8)$$

where B_{sb} is the off diagonal left-handed coupling of Z' boson with quarks and $\mathcal{S}^L_{\ell\ell}$ and $\mathcal{S}^R_{\ell\ell}$ represent the left- and right-handed couplings of Z' boson with leptons, respectively. It is noted here that if a new weak phase ϕ_{sb} is introduced in the off-diagonal coupling B_{sb} then this coupling would read $B_{sb} = |B_{sb}|e^{-i\phi_{sb}}$. One can also write the above equation in the following way

$$\mathcal{H}^{Z'}_{\rm eff} = -\frac{4G_F}{\sqrt{2}}V_{tb}V^*_{ts}[\Lambda_{sb}C_9^{Z'}\mathcal{O}_9 + \Lambda_{sb}C_{10}^{Z'}\mathcal{O}_{10}] + \text{H.c.}, \quad (9)$$

where

$$\Lambda_{sb} = \frac{4\pi e^{-i\phi_{sb}}}{\alpha V^*_{ts}V_{tb}}, \qquad C_9^{Z'} = |B_{sb}|S_{LL}; \qquad C_{10}^{Z'} = |B_{sb}|D_{LL},$$
$$S_{LL} = -(\mathcal{S}^L_{\ell\ell} + \mathcal{S}^R_{\ell\ell}); \qquad D_{LL} = \mathcal{S}^L_{\ell\ell} - \mathcal{S}^R_{\ell\ell}. \quad (10)$$

Thus, to include the Z' into the picture, one has to make the following replacements in the Wilson coefficients C_9 and C_{10}, while, C_7 remains unchanged,

$$C_9^{\rm tot} = C_9^{\rm eff} + \Lambda_{sb}C_9^{Z'}, \qquad C_{10}^{\rm tot} = C_{10} + \Lambda_{sb}C_{10}^{Z'}. \quad (11)$$

The matrix elements in Eq. (3) can be parametrized in terms of form factors as follows [66–72]

$$\langle K^*(k,\varepsilon)|\bar{s}\gamma^\mu(1\pm\gamma^5)b|B(p)\rangle = \mp iq_\mu\frac{2m_{K^*}}{s}\varepsilon^*\cdot q[A_3(s) - A_0(s)] \pm i\varepsilon^*_\mu(m_B + m_{K^*})A_1(s) \mp i(p+k)_\mu\varepsilon^*\cdot q\frac{A_2(s)}{(m_B+m_{K^*})} - \varepsilon_{\mu\nu\lambda\sigma}p^\lambda q^\sigma\frac{2V(s)}{(m_B+m_{K^*})}, \quad (12)$$

$$\langle K^*(k,\varepsilon)|\bar{s}i\sigma_{\mu\nu}q^\nu(1\pm\gamma^5)b|B(p)\rangle = 2\varepsilon_{\mu\nu\lambda\sigma}p^\lambda q^\sigma F_1(s) \pm i\{\varepsilon^*_\mu(m_B^2 - m_{K^*}^2) - (p+k)_\mu\varepsilon^*\cdot q\}F_2(s) \pm i\varepsilon^*\cdot q\left\{q_\mu - \frac{(p+k)_\mu}{(m_B^2 - m_{K^*}^2)}\right\}F_3(s). \quad (13)$$

Contracting above equation by q_μ and using the equation of motion, the form factors $A_3(s)$ can be expressed in terms of the $A_1(s)$ and $A_2(s)$ form factors as follows

$$A_3(s) = \frac{m_B + m_{K^*}}{2mK^*}A_1(s) - \frac{m_B - m_{K^*}}{2mK^*}A_2(s). \quad (14)$$

These seven independent form factors $V(s)$, $A_1(s)$, $A_2(s)$, $A_0(s)$, $F_1(s)$, $F_2(s)$, and $F_3(s)$ are scalar functions of the square of the momentum transfer $s = q^2 = (p-k)^2$ and are nonperturbative quantities. In addition, these form factors are the main source of hadronic uncertainties and have been calculated with different nonperturbative methods such as lattice QCD, quark model (QM) [73], perturbative QCD (PQCD) [74], and light cone-QCD sum rules ($\text{LCSR}_{\rm Old}$) [48], etc. In this regard, to get some rough estimate of how much the double lepton polarization asymmetries are dependent on the choice of the form factors we calculate their average values by using different form factors calculations. However, to extract the information about new physics, we rely on the $\text{LCSR}_{\rm New}$ [75] form factors. These form factors can be parameterized in terms of the square of the momentum transfer as follows. For $\mathbf{LCSR}_{\rm New}$

$$f(s) = \frac{a_1}{1 - s/m_R^2} + \frac{a_2}{1 - s/m_{\rm fit}^2} \quad \text{for } V, A_0 \text{ and } T_1 \quad (15)$$

$$f(s) = \frac{a_1}{1 - s/m_{\rm fit}^2} + \frac{a_2}{(1 - s/m_{\rm fit}^2)^2} \quad \text{for } A_2 \quad \text{and} \quad \tilde{T}_3 \tag{16}$$

$$f(s) = \frac{a_1}{1 - s/m_{\rm fit}^2} \quad \text{for } A_1 \quad \text{and} \quad T_2 \tag{17}$$

where

$$\tilde{T}_3 = T_2 + T3\left(\frac{s}{m_B^2 - m_{K^*}^2}\right).$$

For $\mathbf{LCSR}_{\rm Old}$

$$f(s) = f(0)\exp\left(a_1 \frac{s}{m_B^2} + a_2\left(\frac{s}{m_B^2}\right)^2\right). \tag{18}$$

For **QM**

$$f(s) = \frac{f(0)}{(1 - s/M^2)(1 - a_1 s/M^2 + a_2 s^2/M^4)} \text{for } V, A_0 \text{ and } T_1, \tag{19}$$

$$f(s) = \frac{f(0)}{(1 - a_1 s/M^2 + a_2 s^2/M^4)} \quad \text{for} A_1, A_2, T_2 \text{ and } T_3, \tag{20}$$

where $M = m_B$ for A_0 and $M = m_{B^*}$ for V, A_0, T_1. For the sake of completeness, the values of $f(s)$ at $s = 0$ and a_1, a_2, M, $m_{\rm fit}$ and m_R are listed in Table I and II. For PQCD-I(II), Eq. (19) is used for all form factors. It is worthwhile to mention here that in the literature, FCNC decays have also been studied in the context of the soft collinear effective theory (SCET) at low q^2 (region R_1 in our case) and of a more standard operator product expansion at large q^2 (region R_3 in our case) [76,77]. These approaches are more accurate as they properly take into account the matrix element of operators other than O_7, O_9, and O_{10}.

Now by inserting the matrix elements which are parametrized in terms of the form factors Eqs. (12) and (13) into expression (3), the decay amplitude for $B \to K^* l^+ l^-$ can be written as

$$\begin{aligned}\mathcal{M} = \frac{\alpha G_F}{4\sqrt{2}\pi} V_{tb}^* V_{ts} [&\bar{l}\gamma^\mu(1-\gamma^5)l \times \{-2\mathcal{A}\varepsilon_{\mu\nu\lambda\sigma}\varepsilon^* k^\lambda q^\sigma - i\mathcal{B}_1\varepsilon_\mu^* + i\mathcal{B}_2\varepsilon^*\cdot q(p+k)_\mu + i\mathcal{B}_0\varepsilon^*\cdot q q_\mu\} \\ &+ \bar{l}\gamma^\mu(1+\gamma^5)l \times \{-2\mathcal{C}\varepsilon_{\mu\nu\lambda\sigma}\varepsilon^* k^\lambda q^\sigma - i\mathcal{D}_1\varepsilon_\mu^* + i\mathcal{D}_2\varepsilon^*\cdot q(p+k)_\mu + i\mathcal{D}_0\varepsilon^*\cdot q q_\mu\}],\end{aligned} \tag{21}$$

where the last term in the first line of the above equation will survive only for $\bar{l}\gamma^\mu\gamma^5 l$ due to the fact that $q_\mu(\bar{l}\gamma^\mu\gamma^5 l) = 2m(\bar{l}\gamma^5 l)$ and will vanish for $\bar{l}\gamma^\mu l$ because of $q_\mu(\bar{l}\gamma^\mu l) = 0$. The auxiliary functions $\mathcal{A}$, $\mathcal{C}$, $\mathcal{B}_1$, $\mathcal{D}_1$, $\mathcal{B}_2$ $\mathcal{D}_2$, $\mathcal{B}_0$, and $\mathcal{D}_0$, contain both long and short distance physics which are encapsulated in the form factors and in the Wilson coefficients, respectively, and can be written as follows.

$$\begin{aligned}
\mathcal{A} &= 2C_{LL}\frac{V(s)}{(mB + m_{K^*})} + 4m_b C_7 \frac{F_1(s)}{s}, \\
\mathcal{B}_1 &= 2C_{LL}(mB + m_{K^*})A_1(s) + 4m_b C_7(m_B^2 - m_{K^*})\frac{F_2(s)}{s}, \\
\mathcal{B}_2 &= 2C_{LL}\frac{A_2(s)}{(mB + m_{K^*})} + 4\frac{m_b C_7}{s} \\
&\quad \times \left[F_2(s) + \frac{s}{(m_B^2 - m_{K^*})}F_3(s)\right], \\
\mathcal{B}_0 &= 2m_{k^*}\frac{(A_3 - A_0)}{s} - 4m_b C_7(m_B^2 - m_{K^*})\frac{F_3(s)}{s}, \\
\mathcal{C} &= \mathcal{A}(C_{LL}^{\rightarrow} C_{LR}) \qquad \mathcal{D}_1 = \mathcal{B}_1(C_{LL} \to C_{LR}), \\
\mathcal{D}_2 &= \mathcal{B}_2(C_{LL}^{\rightarrow} C_{LR}) \qquad \mathcal{D}_0 = \mathcal{B}_0(C_{LL} \to C_{LR}),
\end{aligned} \tag{22}$$

where

$$C_{LL} = C_9^{\rm tot} - C_{10}^{\rm tot}, \qquad C_{LR} = C_9^{\rm tot} + C_{10}^{\rm tot}.$$

III. PHYSICAL OBSERVABLES

Now we have all the ingredients to calculate the physical observables. The double differential decay rate is given by [78]

TABLE I. The $\rm LCSR_{New}$ $B \to K^*$ form factors where $f(0)$ denotes the value of form factors at $s = 0$ while a_1, a_2, m_R, and $m_{\rm fit}$ are the parameters in the parametrizations shown in Eq. (18). The typical error in these form factors is 10% which can be reduced up to 6–7%; however, as a conservative estimate we have taken 10% uncertainty in these form factors [75].

$f(s)$	$f(0)$	a_1	a_2	m_R^2	$m_{\rm fit}^2$
$V(s)$	0.411	0.923	−0.511	$m_{1^-}^2$	49.40
$A_1(s)$	0.292	⋯	0.290	⋯	40.38
$A_2(s)$	0.259	−0.084	0.342	⋯	52
$A_0(s)$	0.374	1.364	−0.990	$m_{0^-}^2$	36.78
$F_1(s)$	0.333	0.823	−0.491	$m_{1^-}^2$	46.31
$F_2(s)$	0.333	⋯	0.333	⋯	41.41
$F_3(s)$	0.333	−0.036	0,368	⋯	48.10

TABLE II. $B \to K^*$ form factors where $f(0)$ denotes the value of form factors at $s = 0$ with extrapolating variables a_1 and a_2 in parametrization formula given in Eqs. (18–20) in different QCD approaches.

	$\mathrm{LCSR_{Old}}$			QM			PQCD-I			PQCD-II		
$f(s)$	$f(0)$	a_1	a_2	$f(0)$	a_1	a_2	$f(0)$	a_1	a_2	$f(0)$	a_1	a_2
$V(s)$	0.47	1.482	1.015	0.38	0.66	0.30	0.355	−1.802	0.879	0.332	−1.721	0.744
$A_0(s)$	0.471	1.505	0.710	0.37	0.60	0.16	0.407	−1.282	0.249	381	−1.228	0.148
$A_1(s)$	0.337	0.602	0.258	0.29	0.86	0.60	0.266	−1.034	0.514	0.248	−0.289	0.166
$A_2(s)$	0.282	1.172	0.567	0.26	1.32	0.54	0.202	−1.906	1.168	0.189	−1.801	0.993
$T_1(s)$	0.379	1.510	1.030	0.32	0.66	0.31	0.315	−1.749	0.816	0.294	−0.721	0.202
$T_2(s)$	0.379	0.517	0.426	0.32	0.98	0.90	0.315	−0.975	0.632	0.193	−1.677	0.794
$T_3(s)$	0.260	1.129	1.128	0.23	1.42	0.62	0.207	−1.777	0.964	−0.000	0.001	0.001

$$\frac{d^2\Gamma(B \to K^* l^+ l^-)}{d\cos\theta ds} = \frac{1}{2m_B}\frac{\beta\sqrt{\lambda}}{(8\pi)^3}|\mathcal{M}|^2, \tag{23}$$

where $\beta \equiv \sqrt{1-\frac{4m^2}{s}}$ and $\lambda \equiv m_B^4 + m_{k^*}^4 + s - 2m_B^2 m_{k^*}^2 - 2m_B^2 s - 2m_{k^*}^2 s$. By using the expression of the decay amplitude given in Eq. (21) one can get the expression of the dilepton invariant mass spectrum as

$$\frac{d\Gamma(B \to K^* l^+ l^-)}{ds} = \frac{G_F^2\alpha^2 m_B}{2^{14}\pi^5}|V_{tb}V_{ts}^*|^2\frac{\beta\sqrt{\lambda}}{(8\pi)^3}\Delta, \tag{24}$$

where

$$\begin{aligned}\Delta = 4(2m^2+s)&\left\{\frac{8\lambda}{3}|\mathcal{A}|^2 + \frac{12m_{K^*}^2 s+\lambda}{3m_{K^*}^2 s}|\mathcal{B}_1|^2 - \frac{(m_B^2 - m_{K^*}^2 - s)}{3m_{K^*}^2 s}\mathcal{R}e(\mathcal{B}_1\mathcal{B}_2^*) + \frac{\lambda}{3m_{K^*}^2 s}|\mathcal{B}_2|^2\right\} \\ &+ \frac{32\lambda}{3}(s-4m^2)|\mathcal{C}|^2 + \left[\frac{4\lambda(2m^2+s)}{3m_{K^*}^2 s} + 16(s-4m^2)\right]|\mathcal{D}_1|^2 \\ &- \frac{4\lambda}{3m_{K^*}^2 s}\left\{[(2m^2+s)(m_B^2 - m_{K^*}^2) + s(s-4m^2)]\mathcal{R}e(\mathcal{D}_1\mathcal{D}_2^*) + [6m^2 s(2m_B^2 + 2m_{K^*}^2 - s)\right. \\ &\left. + \lambda(2m^2+s)]|\mathcal{D}_2|^2 + \frac{8m^2\lambda}{m_{K^*}^2}(m_B^2 - m_{K^*}^2)\mathcal{R}e(\mathcal{D}_2\mathcal{D}_0^*) - \frac{8m^2\lambda}{m_{K^*}^2}|\mathcal{D}_0|^2\right\}.\end{aligned} \tag{25}$$

A. Double lepton polarization asymmetries

In this section we will compute the lepton polarization asymmetries in the $B \to K^* l^+ l^-$, i.e., the asymmetries when both of the leptons are simultaneously polarized, namely, the double lepton polarization asymmetries. For this purpose we first define the six orthogonal vectors belonging to the polarization of l^- and l^+ which we denote here by S_i and W_i, respectively, where $i = \mathrm{L}, \mathrm{N}$, and T corresponding to longitudinally, normally, and transversally polarized lepton $l^\pm$, respectively. [79,80]

$$S_L^\mu \equiv (0, \mathbf{e}_L) = \left(0, \frac{\mathbf{p}_-}{|\mathbf{p}_-|}\right), \tag{26}$$

$$S_N^\mu \equiv (0, \mathbf{e}_N) = \left(0, \frac{\mathbf{k}\times\mathbf{p}_-}{|\mathbf{k}\times\mathbf{p}_-|}\right), \tag{27}$$

$$S_T^\mu \equiv (0, \mathbf{e}_T) = (0, \mathbf{e}_N \times \mathbf{e}_L), \tag{28}$$

$$W_L^\mu \equiv (0, \mathbf{w}_L) = \left(0, \frac{\mathbf{p}_+}{|\mathbf{p}_+|}\right), \tag{29}$$

$$W_N^\mu \equiv (0, \mathbf{w}_N) = \left(0, \frac{\mathbf{k}\times\mathbf{p}_+}{|\mathbf{k}\times\mathbf{p}_+|}\right), \tag{30}$$

$$W_T^\mu \equiv (0, \mathbf{w}_T) = (0, \mathbf{w}_N \times \mathbf{w}_L), \tag{31}$$

where p_+, p_-, and k denote the three momenta vectors of the final particles l^+, l^-, and K^*, respectively. The polarization vectors $S_i^\mu(W_i^\mu)$ in Eqs. (26) to (30) are defined in the rest frame of $l^-(l^+)$. When we apply a Lorentz boost to bring these polarization vectors from the rest frame of $l^-(l^+)$ to the center of mass frame of l^+ and l^-, only the longitudinal polarization four vector gets boosted while the other two polarization vectors remain unchanged. After this operation the longitudinal four vectors read

$$S_L^\mu = \left(\frac{|p_-|}{m}, \frac{E_l \mathbf{p}_-}{m|\mathbf{p}_-|}\right), \tag{32}$$

$$W_L^\mu = \left(\frac{|p_+|}{m}, -\frac{E_l \mathbf{p}_+}{m|\mathbf{p}_+|}\right). \tag{33}$$

To obtain the polarization asymmetries one can use the spin projector $\frac{1}{2}(1+\gamma_5 \not{S})$ for l^- and for the l^+, the spin projector is $\frac{1}{2}(1+\gamma_5 \not{W})$.

As we have all the technical tools in our hand, we are in a position to define all the possible lepton polarization asymmetries. Here first we write the single lepton polarization asymmetries formula which is given in [81,82]

$$P_i^\pm = \frac{\frac{d\Gamma(\mathbf{s}^\pm=\hat{\mathbf{i}})}{ds} - \frac{d\Gamma(\mathbf{s}^\pm=-\hat{\mathbf{i}})}{ds}}{\frac{d\Gamma(\mathbf{s}^\pm=\hat{\mathbf{i}})}{ds} + \frac{d\Gamma(\mathbf{s}^\pm=-\hat{\mathbf{i}})}{ds}}, \tag{34}$$

where $\hat{\mathbf{i}}$ denotes the unit vector along L, N, and T and $\mathbf{s}^\pm$ is the spin direction of $l^\pm$. The relation between the polarized and unpolarized invariant dilepton mass spectrum for the $B \to K^* l^+ l^-$ reads

$$\frac{d\Gamma(\mathbf{s}^\pm)}{ds} = \frac{1}{2}\left(\frac{d\Gamma}{ds}\right)[1 + (P_L \mathbf{e}_L + P_N \mathbf{e}_N + P_T \mathbf{e}_T)\cdot \mathbf{s}^\pm]. \tag{35}$$

Besides the single lepton l polarization asymmetries, the asymmetries when both leptons are simultaneously polarized, namely, the double lepton polarization asymmetries can also be observed. Therefore, with three single lepton polarization asymmetries we have nine more double polarization asymmetries which can be helpful to put more strict tests on the SM and to extract possible NP. The double lepton polarization asymmetries read [82,81]:

$$P_{ij} = \frac{[\frac{d\Gamma(\mathbf{s}^+=\hat{\mathbf{i}},\mathbf{s}^-=\hat{\mathbf{j}})}{ds} - \frac{d\Gamma(\mathbf{s}^+=\hat{\mathbf{i}},\mathbf{s}^-=-\hat{\mathbf{j}})}{ds}] - [\frac{d\Gamma(\mathbf{s}^+=-\hat{\mathbf{i}},\mathbf{s}^-=\hat{\mathbf{j}})}{ds} - \frac{d\Gamma(\mathbf{s}^+=-\hat{\mathbf{i}},\mathbf{s}^-=-\hat{\mathbf{j}})}{ds}]}{[\frac{d\Gamma(\mathbf{s}^+=\hat{\mathbf{i}},\mathbf{s}^-=\hat{\mathbf{j}})}{ds} + \frac{d\Gamma(\mathbf{s}^+=\hat{\mathbf{i}},\mathbf{s}^-=-\hat{\mathbf{j}})}{ds}] + [\frac{d\Gamma(\mathbf{s}^+=-\hat{\mathbf{i}},\mathbf{s}^-=\hat{\mathbf{j}})}{ds} + \frac{d\Gamma(\mathbf{s}^+=-\hat{\mathbf{i}},\mathbf{s}^-=-\hat{\mathbf{j}})}{ds}]}. \tag{36}$$

By using the decay rate which is given in Eq. (24) with the polarization vectors defined in Eqs. (26)–(33), we get the following expressions for the double lepton polarization asymmetries

$$\begin{aligned}
P_{LL}(s) = {} & (2m^2 - s)\left(\frac{32\lambda}{3}|\mathcal{A}|^2 + \frac{16\lambda}{3m_{K^*}^2 s}(12m_{K^*}^2 s + \lambda)|\mathcal{B}_1|^2 + \frac{4\lambda^2}{3m_{K^*}^2}|\mathcal{B}_2|^2\right) \\
& + \frac{32\lambda}{3}(4m^2 - s)|\mathcal{C}|^2 + \frac{4\lambda[2m^2\{6(-m_B^2 + m_{K^*}^2 + s)^2 - \lambda\} - s(12m_{K^*}^2 s + \lambda)}{3m_{K^*}^2 s}]|\mathcal{D}_1|^2 \\
& + \frac{2\lambda\{6m^2(m_B^2 - m_{K^*}^2)^2 + \lambda(4m^2 - s)\}}{3m_{K^*}^2 s}|\mathcal{D}_2|^2 + \frac{8m^2 s\lambda}{m_{K^*}^2}|\mathcal{D}_0|^2 + \frac{2\lambda}{3m_{K^*}^2}(2m^2 - s)\mathcal{R}e(\mathcal{B}_1\mathcal{B}_2^*) \\
& - \frac{8m^2 s\lambda}{m_{K^*}^2}\mathcal{R}e(\mathcal{D}_1\mathcal{D}_0^*) + \frac{8m^2\lambda(m_B^2 - m_{K^*}^2)}{m_{K^*}^2}\mathcal{R}e(\mathcal{D}_2\mathcal{D}_0^*) + 2m^2\lambda\{10(m_B^2 + m_{K^*}^2 + s) \\
& - s(6 + m_B^2 - m_{K^*}^2 - s)\}\mathcal{R}e(\mathcal{D}_1\mathcal{D}_2^*),
\end{aligned} \tag{37}$$

$$\begin{aligned}
P_{LN}(s) = {} & \frac{\pi m\sqrt{\lambda}}{m_{K^*}^2\sqrt{s}}[(-m_B^2 + m_{K^*}^2 + s)\{\mathcal{I}m(\mathcal{B}_1\mathcal{D}_1^*) - (m_B^2 - m_{K^*}^2)\mathcal{I}m(\mathcal{B}_1\mathcal{D}_2^*) + s\mathcal{I}m(\mathcal{B}_1\mathcal{D}_0^*\} + \lambda\mathcal{I}m(\mathcal{B}_2\mathcal{D}_1^*) \\
& + \lambda(m_B^2 - m_{K^*}^2)Im(\mathcal{B}_2\mathcal{D}_2^*) + s\lambda\mathcal{I}m(\mathcal{B}_2\mathcal{D}_0^*)],
\end{aligned} \tag{38}$$

$$\begin{aligned}
P_{LT}(s) = {} & 4\pi m\sqrt{\lambda(s - 4m^2)}\left[\mathcal{R}e(\mathcal{A}\mathcal{D}_1^*) + \mathcal{R}e(\mathcal{B}_1\mathcal{C}_1^*) + \frac{(-m_B^2 + m_{K^*}^2 + s)}{m_{K^*}^2 s}[|\mathcal{D}_1|^2 - \frac{s}{2}\mathcal{R}e(\mathcal{D}_1\mathcal{D}_0^*)]\right. \\
& \left. - \frac{\lambda(m_B^2 - m_{K^*}^2)}{2m_{K^*}^2 s}|\mathcal{D}_2|^2 + \frac{2\lambda + s(m_B^2 + m_{K^*}^2 - s)}{4m_{K^*}^2 s}\mathcal{R}e(\mathcal{D}_1\mathcal{D}_2^*) - \frac{\lambda}{4m_{K^*}^2}\mathcal{R}e(\mathcal{D}_2\mathcal{D}_0^*)\right],
\end{aligned} \tag{39}$$

$$P_{TL}(s) = -4\pi m\sqrt{\lambda(s-4m^2)}\Big\{\mathcal{R}e(\mathcal{A}\mathcal{D}_1^*) + \mathcal{R}e(\mathcal{B}_1\mathcal{C}_1^*) + \frac{(m_B^2 - m_{K^*}^2 - s)}{2m_{K^*}^2 s}[|\mathcal{D}_1|^2 - \frac{s}{2}\mathcal{R}e(\mathcal{D}_1\mathcal{D}_0^*)] - \frac{2\lambda + s(m_B^2 + m_{K^*}^2 - s)}{4m_{K^*}^2 s}\mathcal{R}e(\mathcal{D}_1\mathcal{D}_2^*) + \frac{\lambda(m_B^2 - m_{K^*}^2)}{2m_{K^*}^2 s}|\mathcal{D}_2|^2 + \frac{\lambda}{4m_{K^*}^2}\mathcal{R}e(\mathcal{D}_2\mathcal{D}_0^*)\Big\}, \tag{40}$$

$$P_{NL}(s) = -P_{LN}(s), \tag{41}$$

$$P_{NN}(s) = \frac{16\lambda}{3}(s-4m^2)(|\mathcal{A}|^2 - |\mathcal{C}|^2) - \left(\frac{4\lambda(2m^2+s)}{3m_{K^*}^2} - 16m^2\right)|\mathcal{B}_1|^2 + \frac{4\lambda}{3m_{K^*}^2}[(2m^2+s)\{(m_B^2 - m_{K^*}^2 - s)\mathcal{R}e(\mathcal{B}_1\mathcal{B}_2^*) + |\mathcal{D}_1|^2\} + \{(m_B^2 - m_D^2)(2m^2+s) + s(s-4m^2)\}\mathcal{R}e(\mathcal{D}_1\mathcal{D}_2^*) - 6m^2 s\mathcal{R}e(\mathcal{D}_1\mathcal{D}_0^*) + \{6m^2 s(2m_B^2 + 2m_{K^*}^2 - s) + \lambda(2m^2+s)\}|\mathcal{D}_2|^2 + 6m^2 s(m_B^2 - m_{K^*}^2)\mathcal{R}e(\mathcal{D}_2\mathcal{D}_0^*) + 6m^2 s^2 m_{K^*}^2|\mathcal{D}_0|^2], \tag{42}$$

$$P_{NT}(s) = \lambda\sqrt{s-4m^2}\left[\frac{16}{3}\mathcal{I}m(\mathcal{A}\mathcal{C}_1^*) - \frac{4}{3m_{K^*}^2\sqrt{s}}\{\mathcal{I}m(\mathcal{B}_1\mathcal{D}_1^*) - (m_B^2 - m_{K^*}^2 - s)(\mathcal{I}m(\mathcal{B}_1\mathcal{D}_2^*) + \mathcal{I}m(\mathcal{B}_2\mathcal{D}_1^*)) - \lambda\mathcal{I}m(\mathcal{B}_2\mathcal{D}_2^*)\}\right], \tag{43}$$

$$P_{TN}(s) = -P_{NT}(s), \tag{44}$$

$$P_{TT}(s) = \frac{16\lambda}{3}[(4m^2+s)|\mathcal{A}|^2 + (4m^2-s)|\mathcal{C}|^2] + \left\{16m^2 - \frac{2\lambda(s-2m^2)}{3m_{K^*}^2 s}\right\}|\mathcal{B}_1|^2 + \frac{4\lambda}{3m_{K^*}^2 s}[(s-2m^2)(m_B^2 - m_{K^*}^2 - s)\mathcal{R}e(\mathcal{B}_1\mathcal{B}_2^*) - \lambda(s-2m^2)|\mathcal{B}_2|^2 + (s-10m^2)|\mathcal{D}_1|^2 + \{(10m^2 - s)(m_B^2 - m_{K^*}^2) - s(4m^2 - s)\}\mathcal{R}e(\mathcal{D}_1\mathcal{D}_2^*) + 6m^2 s\mathcal{R}e(\mathcal{D}_1\mathcal{D}_0^*) + \{\lambda(s-10m^2) - 6m^2 s(2m_B^2 + 2m_{K^*}^2 - s)\}|\mathcal{D}_2|^2 - 6m^2 s(m_B^2 - m_{K^*}^2)\mathcal{R}e(\mathcal{D}_2\mathcal{D}_0^*) - 6m^2 s^2|\mathcal{D}_0|^2]. \tag{45}$$

It is important here to mention that the SM expression obtained for the lepton polarization asymmetries match the results of Ref. [83]. It is noted here that the explicit expressions of double lepton polarization asymmetries listed in Eqs. (37–45), respectively, are functions of s and at the Z' model's parameters B_{sb}, S_{LL}, D_{LL}, and ϕ_{sb}. Now, to see the explicit dependence on the new physics parameters we have to integrate these polarization asymmetries over s to obtain the average values of these asymmetries. Therefore, we also calculate the averaged asymmetries by using the following formula

$$\langle P_i\rangle = \frac{\int_{4m^2}^{(m_B^2 - m_{k^*}^2)} P_i \frac{d\Gamma}{ds} ds}{\int_{4m^2}^{(m_B^2 - m_{k^*}^2)} \frac{d\Gamma}{ds} ds}. \tag{46}$$

IV. PHENOMENOLOGICAL ANALYSIS AND DISCUSSION

In this section we present the new physics effects on the various lepton polarization asymmetries. Before we start the phenomenological analysis, first we want to give numerical values of the different parameters which are involved in the calculation of the polarization asymmetries. For this purpose the form factors of $B \to K^*$ are given in Table I and II. The masses and other parameters are listed in Table III and the SM Wilson coefficients at $\mu = m_b$ are given in Table IV.

Now to pursue the investigation of Z' effects in the lepton polarization asymmetries for $B \to k^* l^+ l^-$, it is interesting to see how much these lepton polarization asymmetries are affected by the particular choice of the form factors. To

TABLE III. Default values of input parameters used in the calculations [84].

$m_B = 5.28$ GeV, $m_b = 4.28$ GeV, $m_\mu = 0.105$ GeV, $m_\tau = 1.77$ GeV, $f_B = 0.25$ GeV, $\lvert V_{tb}V_{ts}^*\rvert = 45 \times 10^{-3}$, $m_{B^*} = 5.37$, $\alpha^{-1} = 137$, $G_F = 1.17 \times 10^{-5}$ GeV^{-2}, $\tau_B = 1.54 \times 10^{-12}$ sec, $m_{K^*} = 0.892$ GeV.

achieve this purpose, we have chosen four form factors, namely (i) $\mathrm{LCSR_{New}}$ (ii) $\mathrm{LCSR_{Old}}$ (iii) PQCD(I&II), and (iv) QCD and tabulated the average values of double lepton polarization asymmetries in Tables VII VIII within the SM and XI X&XI with (without) including the long distance effects in Z' model. From these average values one can see that results from PQCD(I&II) overlap but differ from QM and LCSR results which are close to each other, so, in general, we can say that some of these lepton polarization asymmetries are sensitive to the choice of the form factors. However, to analyze the new physics effects of Z' on these asymmetries, we rely on the latest results of light cone QCD sum rules (LCSR) form factors and, for the comparison, their average values are also calculated using PQCD(I&II)

It is worthwhile to mention that in Figs. 1 and 2, the thick solid line corresponds to the SM value of the polarization asymmetries. Here one can notice that the uncertainty in the values of the asymmetries due to the hadronic form factors are negligible. Yellow and pink regions depict the variation in the values of the asymmetries when Z' boson effects are taken into account and for these regions the values of different parameters of Z' model are described in the chart given below. Similarly, the corresponding values of Z' parameters for the color region scheme of the graphs of average values $\langle P_{ij}\rangle$ presented in Figs. 3–6 are listed in Table V.

color Regions for Figs. 1 × and 2				
s-dependence graphs	ϕ_{sb}	S_{LL}	D_{LL}	B_{sb}^L
Yellow	$-75^\circ - -65^\circ$	$-6.7 - +1.1$	$-9.3 - -4.1$	$+1.31 - +0.87$
Pink	$-86^\circ - -78^\circ$	$-2.6 - +0.2$	$-2.34 - -1.6$	$+2.35 - +2.05$

A. New physics in double lepton polarization asymmetry

To see how much lepton polarization asymmetries are impacted by an extra Z' gauge boson, we have plotted these lepton polarization asymmetries against the square of the momentum transfer s in Figs. 1a–1f and in Figs. 2a–2g for muons and taus, respectively. In these plots we have chosen the numerical values of coupling parameters of the Z' model within the ranges of two different fits of B_s-$\bar{B}_s$ mixing data by the UTfit collaboration [86] that are listed in Table VI. As we have mentioned earlier, the value of these polarization asymmetries are negligibly effected from the uncertainties in the hadronic form factors, therefore, these uncertainties do not preclude us to see the NP effects of an extra gauge boson in these asymmetries. To get more insight about the variation in the values of various lepton polarization asymmetries due to the presence of an extra gauge boson, we have also computed their average values and have plotted these values against S_{LL} (D_{LL}) in Figs. 3 (4) for muons and in Figs. 5 (6) for taus. In addition, in Tables VII (VIII) we present the average values of these asymmetries in the SM calculated using the central values of the form factors and without (with) the inclusion of long distance effects. Similarly, the numerical values of $\langle P_{ij}\rangle$ in Z' model without including LD effects are given in Tables XI while the results obtained including LD effects are given in Tables X and XI. In these tables, scenarios I and II are taken from Ref. [87] which presents the allowed Z' parameters' ranges to get the smallest values of $\mathcal{B}(\bar{B} \to \phi\mu^+\mu^-)$ and $A_{FB}(\bar{B} \to \phi\mu^+\mu^-)$, respectively. For completeness and convenience these scenarios are given below

$$B_{sb} = 1.31, \quad \varphi_{sb} = -65^\circ, \quad S_{LL} = -2, \quad D_{LL} = -4 \quad \text{Scenario I}$$
$$B_{sb} = 1.31, \quad \varphi_{sb} = -65^\circ, \quad S_{LL} = 1.1, \quad D_{LL} = -9.3 \quad \text{Scenario II}$$

TABLE IV. The Wilson coefficients C_i^μ at the scale $\mu \sim m_b$ in the SM [85].

C_1	C_2	C_3	C_4	C_5	C_6	C_7	C_9	C_{10}
1.107	−0.248	−0.011	−0.026	−0.007	−0.031	−0.313	4.344	−4.669

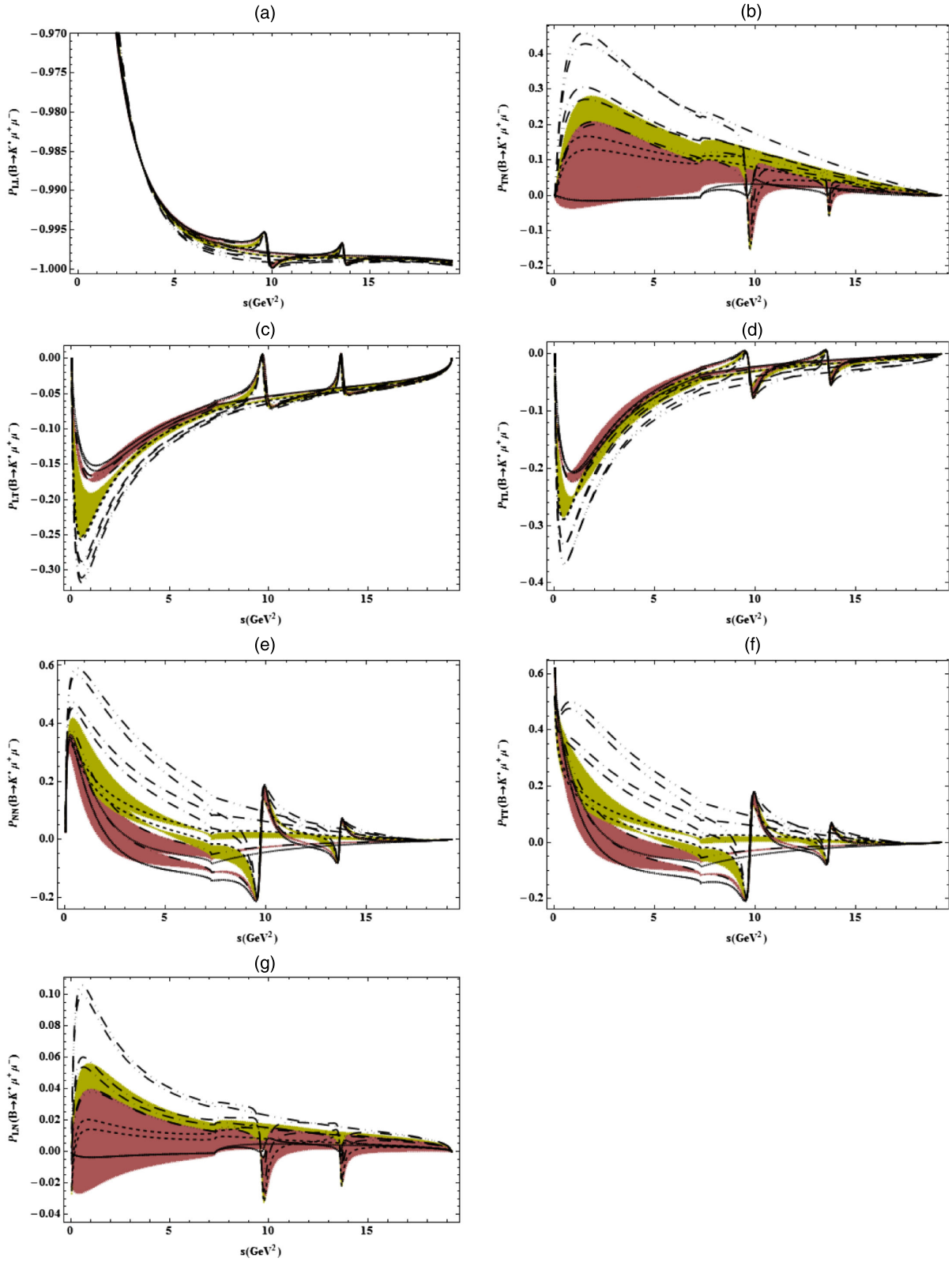

FIG. 1 (color online). The dependence of double lepton polarization asymmetries for the decay $B \to K^*(892)l^+l^-$ on s. The first column for the $\mu^+\mu^-$ and the second column for the $\tau^+\tau^-$. Dashed, dashed dotted, and dashed double dotted correspond to curves with $B_{sb} = 1.31$, $D_{LL} = -9.3$, $S_{LL} = -6.3, -3, +1.1$, and $\varphi_{sb} = -79°, -72°, -65°$, respectively. Dashed triple dotted line correspond to $B_{sb} = +2.05$, $D_{LL} = -1.16$, $S_{LL} = +0.2$, and $\phi_{sb} = -78°$. Solid lines represent the SM values of the asymmetries and features of the other color regions are described in the text just above Table V.

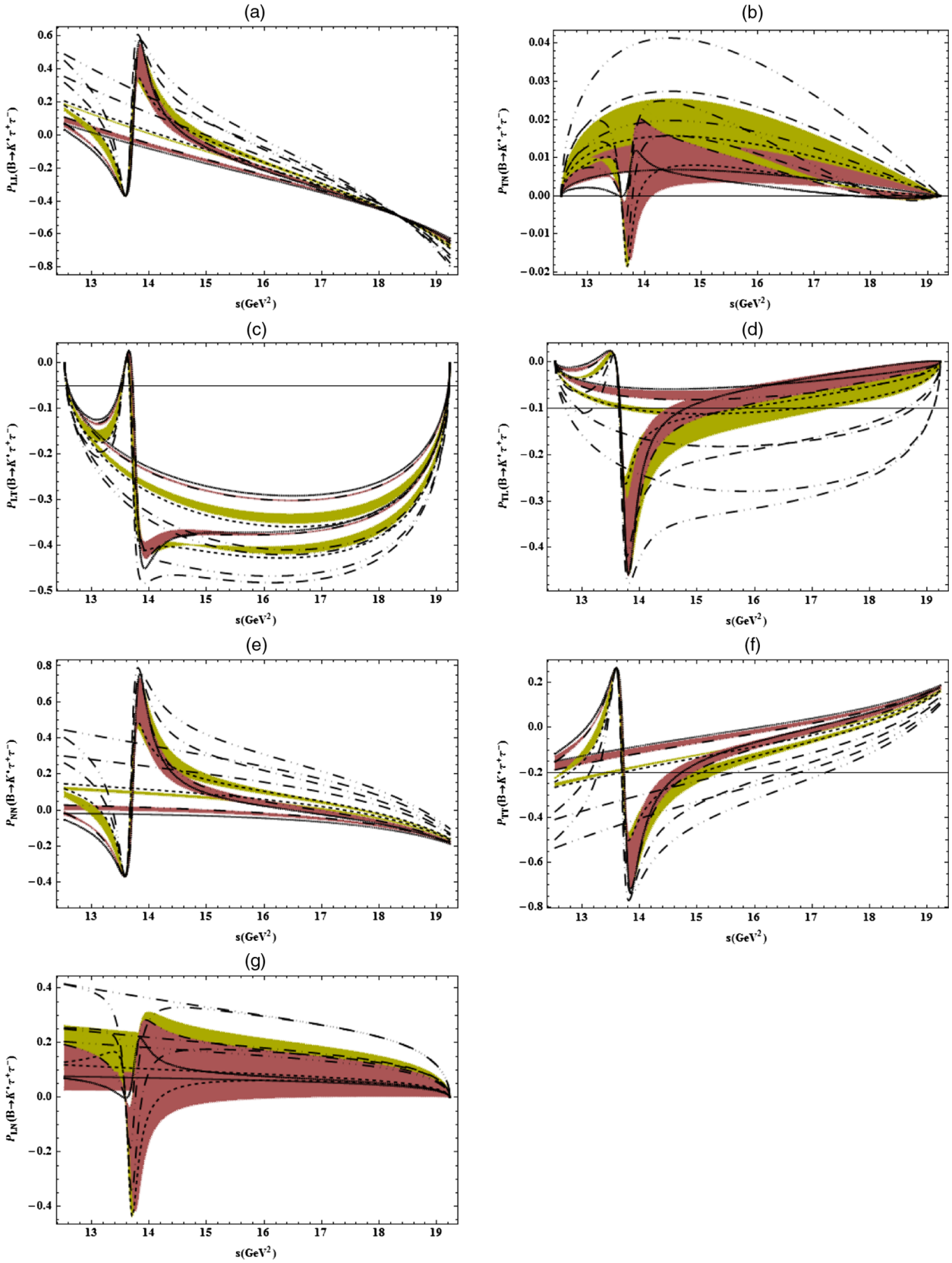

FIG. 2 (color online). Legends are the same as in Fig. 1 but for double lepton polarization asymmetries P_{ij} when taus are the final state leptons.

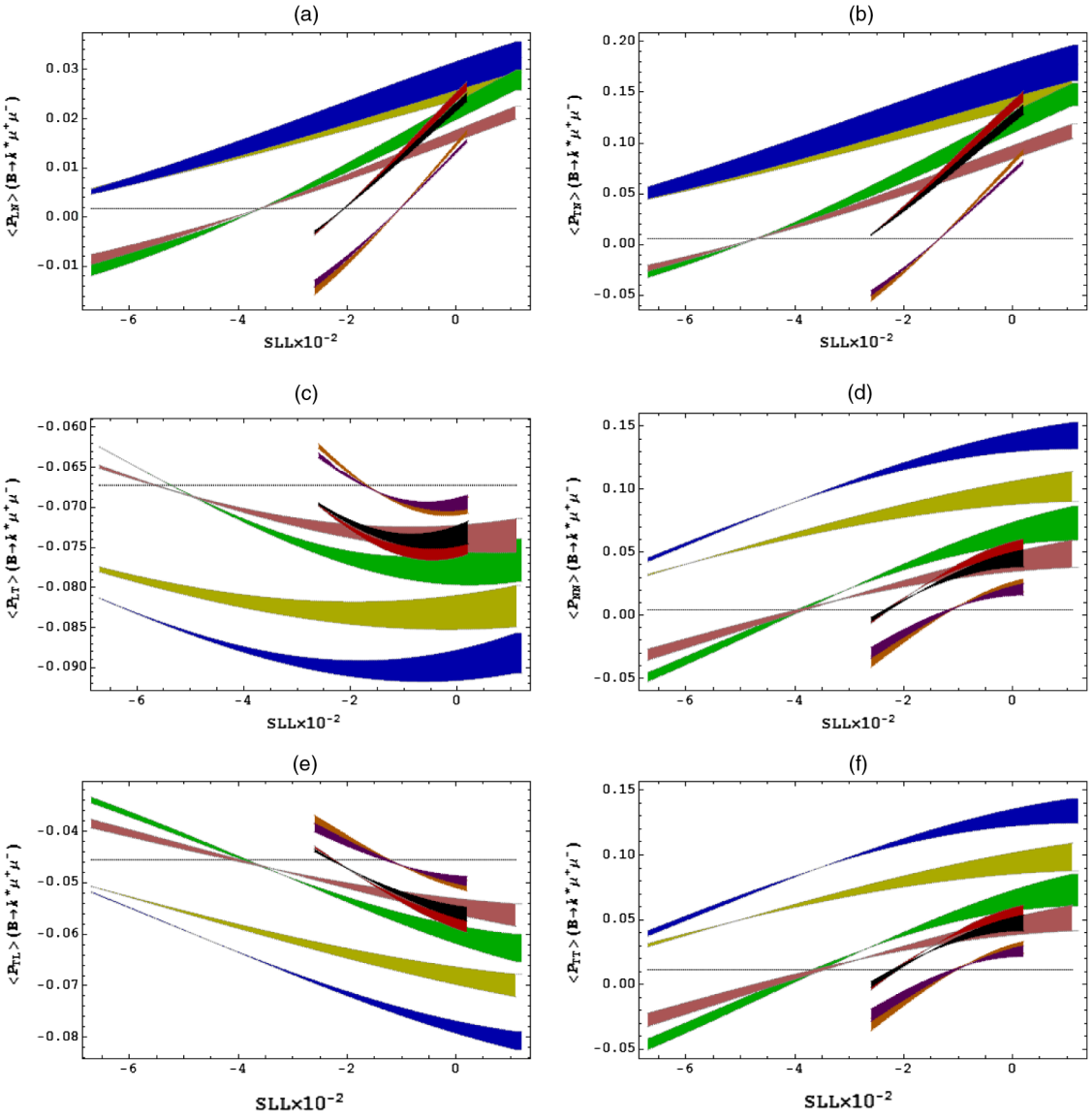

FIG. 3 (color online). The dependence of average values of double lepton polarization asymmetries $\langle P_{ij}\rangle$ for the decay $B \to K^*(892)l^+l^-$ on S_{LL} in S_1 and S_2, for the $\mu^+\mu^-$ case. Solid line represents the SM value of asymmetry and features of the other color regions are described in the text above in Table V.

To determine the average values of $\langle P_{ij}\rangle$ with long distance effects, we have included only two resonances, namely J/ψ and ψ', and introduced three regions R_i as discussed in [88].

For $\ell = \mu$

$$\mathrm{R}_1:\ 2m_\mu \le \sqrt{s} \le M_{J/\psi} - 0.20;$$
$$\mathrm{R}_2:\ M_{J/\psi} + 0.04 \le \sqrt{s} \le M_{\psi'} - 0.10;$$
$$\mathrm{R}_3:\ M_{\psi'} + 0.02 \le s \le m_{B_s} - m_{K^*}.$$

For $\ell = \tau$, region R_3 is similar but R_2 becomes

$$\mathrm{R}_2:\ 2m_\tau \le \sqrt{s} \le M_{\psi'} - 0.10.$$

Now we begin to discuss the phenomenological analysis of the impact of the Z' model on the double lepton polarization asymmetries and their average values denoted by P_{ij} and $\langle P_{ij}\rangle$, respectively, for $B \to K^* l^+ l^-$ decays, where $l = \mu, \tau$. Before beginning, it should be noted here that $P_{NT} = -P_{TN}$ and $P_{LN} = -P_{NL}$. It is also found that the SM values of P_{TN} for both muons and taus and P_{LN} only for muons are tiny to measure but these values get large in the presence of the Z' boson; therefore, any measurement of these asymmetries is clear evidence of new physics. However, the other double lepton polarization asymmetries that are sensitive to NP are discussed in the following.

(i) The double lepton polarization asymmetry P_{LL} as a function of s in the SM and in the Z' model by using

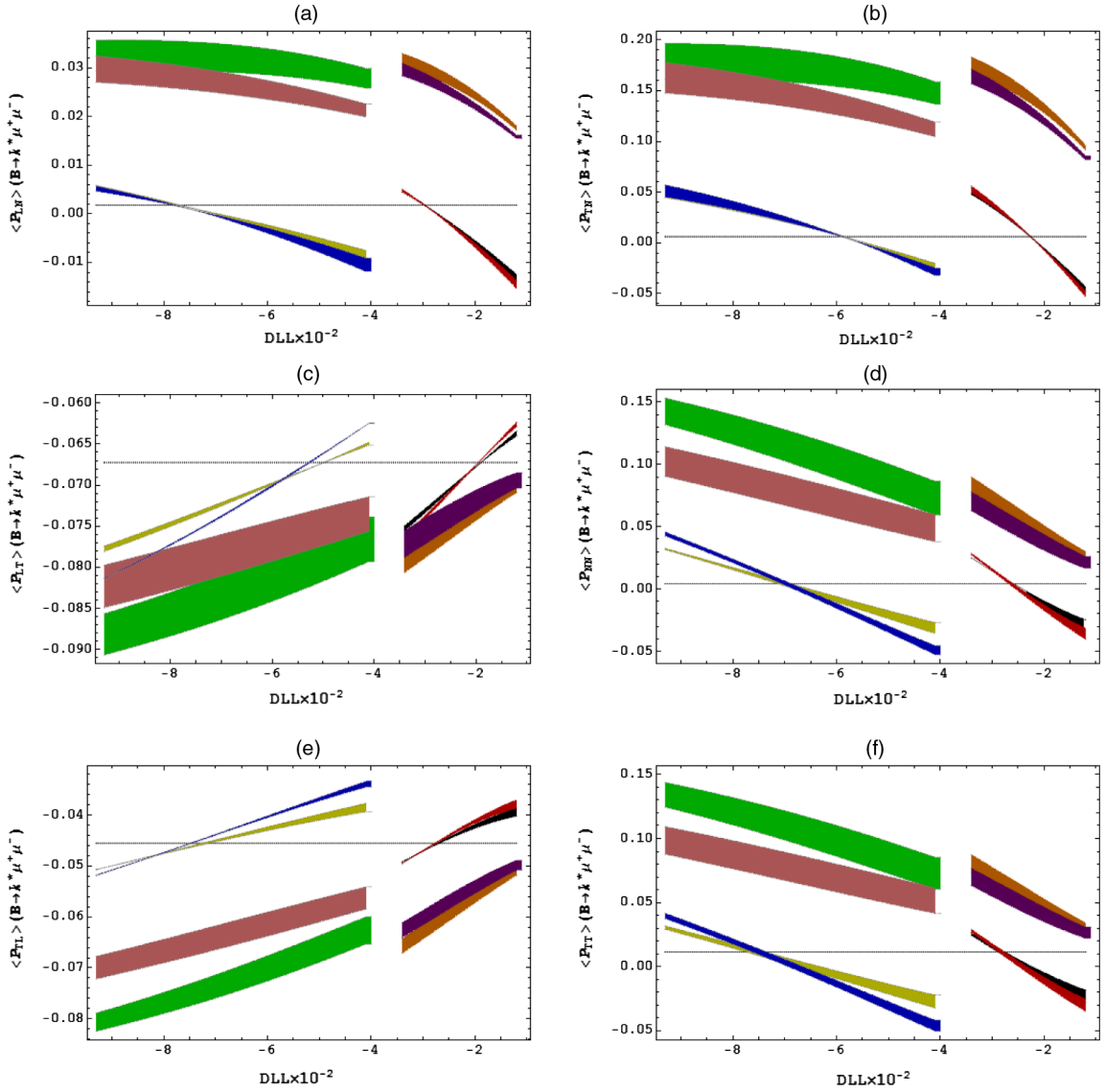

FIG. 4 (color online). The dependence of average values of double lepton polarization asymmetries $\langle P_{ij} \rangle$ for the decay $B \to K^*(892) l^+ l^-$ on D_{LL} in S_1 and S_2, for the $\mu^+\mu^-$ case. Solid line represents the SM value of asymmetry and features of the other color regions are described in the text above in Table V.

different values of new physics parameters with and without resonance effects is shown in Figs. 1a and 2a for the case of muons and taus, respectively. It can easily be seen from Fig. 1a which is the case of muons, that P_{LL} is an increasing function of s, and that at high s its value approaches one. However, the value of P_{LL} is almost insensitive to the new physics parameters, therefore, it does not provide any information about the extra gauge boson physics. On the other hand, when taus are the final state leptons, P_{LL} depends on the choice of the form factors as one can see from Table VII, where, for LCSR_{NeW} form factors the average value $\langle P_{LL} \rangle$ is approximately -0.249 while for PQCD form factors $\langle P_{LL} \rangle$ is -0.429. Moreover, from Fig. 2a it can also be seen that P_{LL} is an increasing function throughout the s region and its value varies from $+0.06$ at s_{min} to -0.65 at s_{max}. Furthermore, in contrast to the case of muons, the new physics effects are also prominent and at some values of new physics parameters, its minimum SM value $+0.06$ at s_{min} is enhanced up to $+0.5$. However, the maximum value at s_{max} does not change much.

(ii) Similarly, the s dependence of P_{LT} and P_{TL} (for muons) is displayed in Figs 1c and 1d, respectively. One can find from these figures that the behavior of these asymmetries as a function of s in the SM and in presence of a Z' boson is almost the same, i.e., both of these asymmetries are a decreasing function of s. In the presence of an extra gauge boson the maximum value of these asymmetries is significantly shifted. As

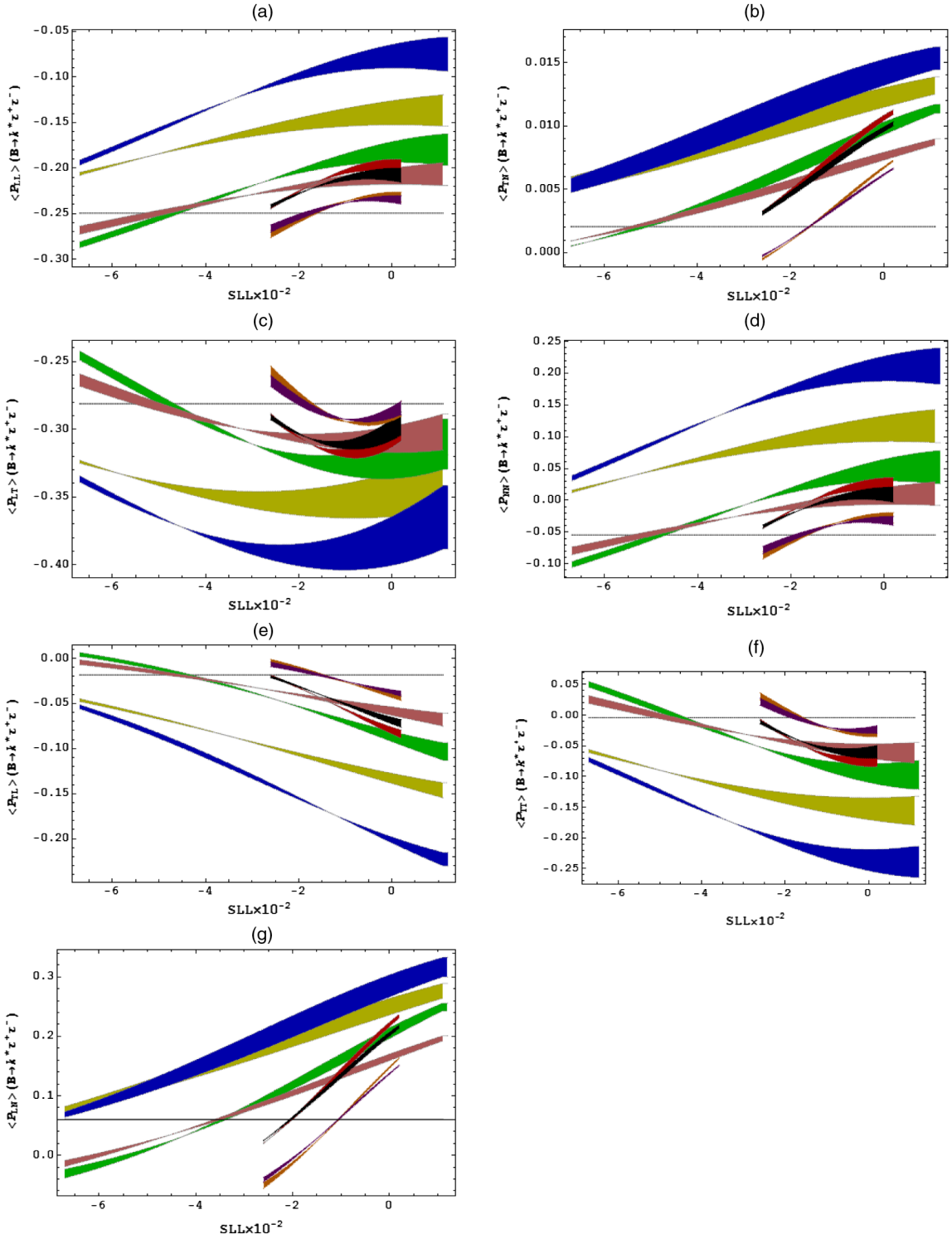

FIG. 5 (color online). Legends are the same as in Fig. 3 but for average double lepton polarization asymmetries $\langle P_{ij} \rangle$ when taus are the final state leptons.

one can see from these figures, the SM value of $P_{LT(TL)} \approx -0.15$ (-0.20) is shifted to -0.32 (-0.36) when we set $B_{sb} = +2.05$, $D_{LL} = -1.16$, $S_{LL} = +0.2$ and $\phi_{sb} = -78^\circ$. Similarly, for the case of taus these asymmetries as a function of s are displayed in Figs. 2c and 2d, whereupon one can see the effects on these asymmetries due to the extra gauge boson are prominent throughout the s region. Furthermore, one can deduce from Fig. 2c (2d) that the maximum value of P_{TL} (P_{LT}) in the SM without including large

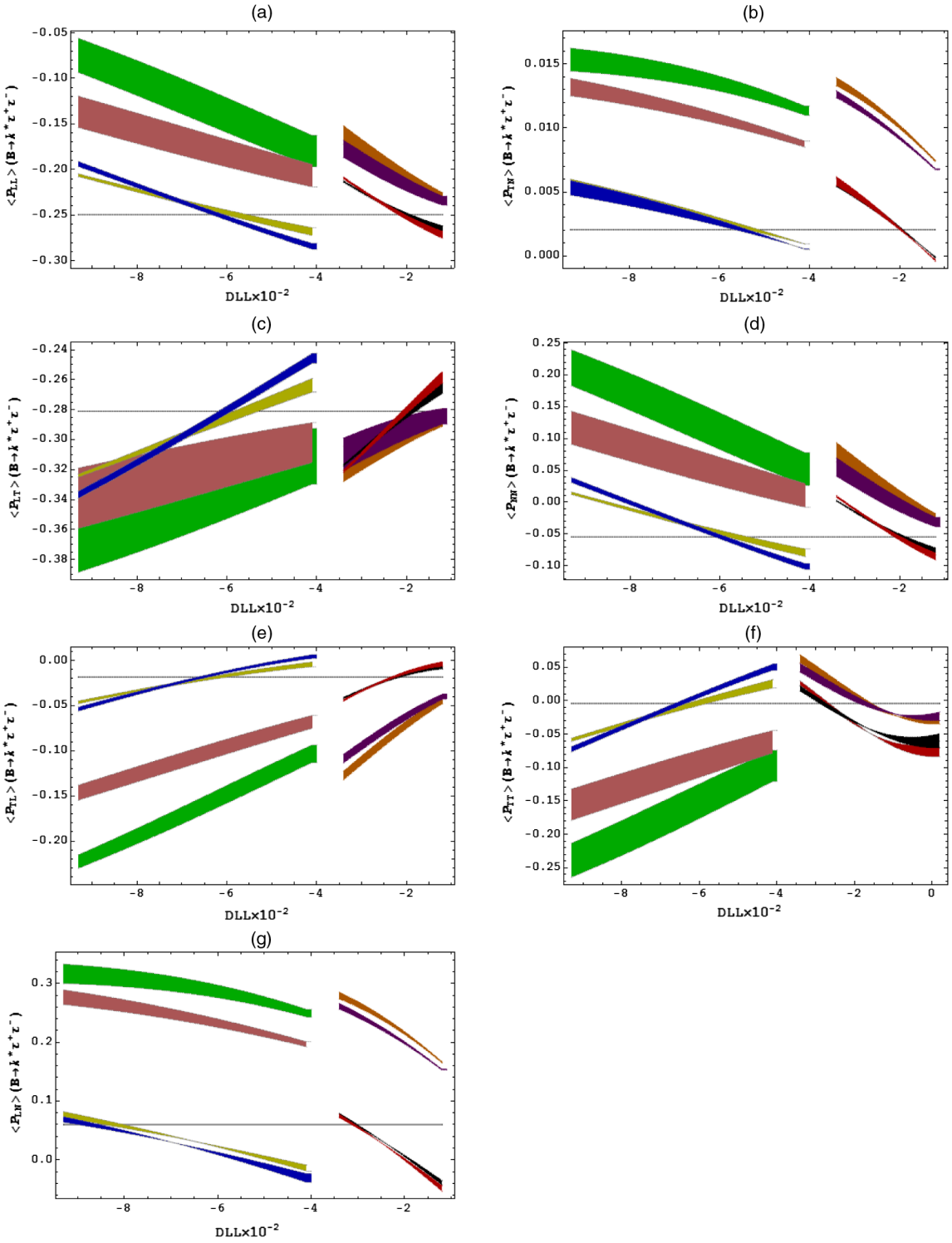

FIG. 6 (color online). Legends are the same as in Fig. 4 but for average double lepton polarization asymmetries $\langle P_{ij} \rangle$ when taus are the final state leptons.

distance effects is -0.3 (-0.05) and in the presence of an extra gauge boson it raises up to -0.42 (-0.28) with $B_{sb} = +1.31$, $D_{LL} = -9.3$, $S_{LL} = +1.1$, and $\phi_{sb} = -65^\circ$ (see the dashed double dotted line in these graphs).

(iii) The average values of P_{LT} and P_{TL} for the case of muons/taus are drawn in Figs. 3c, 5c (4c, 6c) and Figs. 3e, 5e (4e, 6e) vs S_{LL} (D_{LL}) both for S1 and S2. These graphs show that almost the extra gauge boson effects on these asymmetries are decreasing

TABLE V. Color region scheme for Figs. $\langle P_{ij}\rangle$ vs S_{LL} and D_{LL}.

Color Region	ϕ_{sb}	B_{sb}	$\langle P_i\rangle$ and $\langle P_{ij}\rangle$ vs S_{LL} D_{LL}	$\langle P_i\rangle$ and $\langle P_{ij}\rangle$ vs D_{LL} S_{LL}
Blue	-79° -65°	+1.31	−9.3	−6.7
Red	-86° -78°	+2.35	−2.34	−2.6
Yellow	-79° -65°	+0.87	−9.3	−6.7
Black	-86° -78°	+2.05	−2.34	−2.6
Green	-79° -65°	+1.31	−4.1	+1.1
Brown	-86° -78°	+2.35	−1.16‘	+0.2
Pink	-79° -65°	+0.87	−4.1	+1.1
Purple	-86° -78°	+2.05	−1.16	+0.2

TABLE VI. The numerical values of the $Z\prime$ parameters [14,86].

	$\mathcal{R}e(B_{sb})\times 10^{-3}$	φ_{sb}(in Degree)	$S_{LL}\times 10^{-2}$	$D_{LL}\times 10^{-2}$
$S1$	1.09 ± 0.22	-72 ± 7	-2.8 ± 3.9	-6.7 ± 2.6
$S2$	2.20 ± 0.15	-82 ± 4	-1.2 ± 1.4	-2.5 ± 0.9

(increasing) function of D_{LL} (S_{LL}) and enhance (reduce) the values of these asymmetries. It is found from Figs. 3c and 3e for muons [5c and 5e for taus] that the maximum deviation from the SM value of $P_{LT}=-0.067$ [−0.281] is about 27.17% (12.42%) [31.46%(12.19%)] for S1 (S2) at $S_{LL}=-0.05$ while for $P_{TL}=-0.043$ [−0.02] the maximum deviation is about 47.56% (28.33%) [91.30% (77.78%)] for S1 (S2) at $S_{LL}=+1.1$ ($S_{LL}=+0.2$). Similarly, one can notice from Figs. 4c and 4e for muons [6c and 6e for taus] that the maximum deviation in the value of P_{TL} is 27.17% (18.29%) [28.20% (13.85%)] at $D_{LL}=-9.3$ (−3.4) and for P_{TL} the maximum deviation is 47.56% (35.82%) [91.30% (84.61%)] for S1 (S2). One can also see the sensitivity of these observables on the choice of form factors from Table VII.

(iv) From the new physics point of view of an extra gauge boson Z' model, P_{TN} is also very sensitive as we have plotted these asymmetries in Figs. 1b and 2b for the case of muons and taus, respectively, as a function of s in SM and in the Z' model. It is already mentioned above that in the SM, the values of these asymmetries are not in a measurable range, thereupon, measurement of these asymmetries provide a clear signature of new physics. Furthermore, in the context of an extra gauge boson one can immediately see by these graphs, particularly for the case of muons, that in the low s region the effects are more prominent and approximately at 8 GeV^2 its value reaches up to $\approx +0.45$. Additionally, the magnitude of these asymmetries also provide some stringent constraints on the different parameters of the Z' model. For instance, the value of P_{TN} for the case of muons changes roughly from 0 to +0.5 in the region $1\le s\le 5$ GeV^2 for different values of the Z' model parameters.

(v) The explicit dependence of the average values of P_{TN} on S_{LL} and D_{LL} for muons (taus) with the whole range of new weak phase ϕ_{sb} and B_{sb} are also presented in Figs. 3b 5b and 4b 6b, respectively, both for S1 and S2. Whereupon, it can be seen that, though the change in the values of P_{TN} for taus in the presence of a Z' boson is approximately one order of magnitude smaller than the case of muons, this deviation is still in a measurable range. For example one can see from Figs. 3b and 4b for muons that the maximum value of $\langle P_{TN}\rangle$ in the Z' model is around +0.20 while from Figs. 5b and 6b for taus, it is around +0.016.

(vi) Similar to the case of P_{TN}, P_{LN} for muons is also very tiny in the SM and is significantly affected for various values of the Z' model's parameters. One can see from Fig. 1g for the case of muons as final state leptons that the value of P_{LN} in the low s region raises up to +0.10 due to the influence of the Z' boson. In the same way

TABLE VII. Numerical values of $\langle P_{ij}\rangle$ in the SM without long distance (LD) effects.

	LCSR_{New}		LCSR_{Old}		QM		PQCD-I and II	
$\langle P_{ij}\rangle$	$\mu^+\mu^-$	$\tau^+\tau^-$	$\mu^+\mu^-$	$\tau^+\tau^-$	$\mu^+\mu^-$	$\tau^+\tau^-$	$\mu^+\mu^-$	$\tau^+\tau^-$
$\langle P_{LL}\rangle$	−0.970	−0.249	−0.968	−0.259	−0.976	−0.337	−0.975	−0.429
$\langle P_{LN}\rangle$	0.001	0.060	0.001	0.057	0.002	0.053	0.000	0.041
$\langle P_{NL}\rangle$	−0.001	−0.057	−0.001	−0.057	−0.002	−0.053	−0.000	−0.041
$\langle P_{LT}\rangle$	−0.067	−0.281	−0.075	−0.293	−0.062	−0.280	−0.083	−0.158
$\langle P_{TL}\rangle$	−0.045	−0.018	−0.056	−0.015	−0.042	−0.016	−0.086	−0.046
$\langle P_{TT}\rangle$	0.011	−0.004	0.010	−0.010	0.013	0.027	0.089	0.034
$\langle P_{NN}\rangle$	0.004	−0.054	0.006	−0.057	0.008	−0.122	0.076	−0.319
$\langle P_{TN}\rangle$	0.006	0.002	0.004	0.003	0.004	0.002	0.000	0.001
$\langle P_{NT}\rangle$	−0.004	−0.003	−0.004	−0.003	−0.004	−0.002	−0.000	−0.001

TABLE VIII. Numerical values of $\langle P_{ij}\rangle$ in the SM with long distance (LD) effects.

		LCSR_{New}			LCSR_{Old}			QM			PQCD-I(II)		
$\langle P_{ij}\rangle$		R_1	R_2	R_3	R_1	R_2	R_3	R_1	R_2	R_3	R_1	R_2	R_3
$\langle P_{LL}\rangle$	$\mu^+\mu^-$	−0.939	−0.996	−0.997	−0.939	−0.996	−0.997	−0.945	−0.996	−0.998	−0.930	−0.998	−0.999
	$\tau^+\tau^-$	⋯	−0.016	−0.237	⋯	−0.012	−0.262	⋯	−0.066	−0.354	⋯	−0.216	−0.488
$\langle P_{LN}\rangle$	$\mu^+\mu^-$	−0.001	0.005	0.003	−0.001	0.005	0.003	−0.001	0.005	0.003	−0.002	0.004	0.002
	$\tau^+\tau^-$	⋯	0.064	0.077	⋯	0.063	0.071	⋯	0.062	0.068	⋯	−0.052	−0.052
$\langle P_{NL}\rangle$	$\mu^+\mu^-$	0.001	−0.005	−0.003	0.001	−0.005	−0.003	0.001	−0.005	−0.003	0.002	−0.004	−0.002
	$\tau^+\tau^-$	⋯	−0.064	−0.077	⋯	−0.063	−0.071	⋯	−0.062	−0.068	⋯	0.052	0.052
$\langle P_{LT}\rangle$	$\mu^+\mu^-$	−0.091	−0.054	−0.037	−0.102	−0.056	−0.037	−0.091	−0.050	−0.032	−0.095	−0.036	−0.019
	$\tau^+\tau^-$	⋯	−0.088	−0.351	⋯	−0.095	−0.364	⋯	−0.093	−0.347	⋯	−0.065	−0.212
$\langle P_{TL}\rangle$	$\mu^+\mu^-$	−0.085	−0.022	−0.008	−0.098	−0.025	−0.008	−0.086	−0.022	−0.007	−0.102	−0.024	−0.009
	$\tau^+\tau^-$	⋯	−0.011	−0.062	⋯	−0.015	−0.058	⋯	0.015	−0.057	⋯	−0.026	−0.086
$\langle P_{TT}\rangle$	$\mu^+\mu^-$	0.0002	0.004	−0.005	−0.006	0.004	−0.005	−0.009	0.027	0.018	0.039	0.128	0.091
	$\tau^+\tau^-$	⋯	−0.079	−0.065	⋯	−0.115	−0.064	⋯	−0.075	−0.012	⋯	−0.096	0.052
$\langle P_{NN}\rangle$	$\mu^+\mu^-$	−0.017	0.005	−0.005	−0.015	0.006	−0.005	−0.021	0.028	0.018	0.022	0.128	0.091
	$\tau^+\tau^-$	⋯	−0.082	0.029	⋯	−0.060	0.021	⋯	−0.172	−0.044	⋯	−0.490	−0.201
$\langle P_{TN}\rangle$	$\mu^+\mu^-$	0.005	−0.025	−0.004	0.006	−0.023	−0.004	0.005	−0.033	−0.014	0.008	−0.081	−0.050
	$\tau^+\tau^-$	⋯	−0.002	−0.002	⋯	−0.002	−0.002	⋯	−0.003	−0.008	⋯	−0.009	−0.032
$\langle P_{NT}\rangle$	$\mu^+\mu^-$	−0.005	0.025	0.004	−0.006	0.023	0.004	−0.005	0.033	0.014	−0.008	0.081	0.050
	$\tau^+\tau^-$	⋯	0.002	0.002	⋯	0.002	0.002	⋯	0.003	0.008	⋯	0.009	0.032

for the case of taus, which is described in Fig. 2g, the maximum SM value of P_{LN} is about $+0.07$ at $s = 4m_\tau^2$ and at the same value of s, due to the presence of extra gauge Z' boson, it is increased up to $+0.4$ when we set the values of model's parameters as $B_{sb} = +1.1$, $D_{LL} = -9.3$, $S_{LL} = +1.1$ and $\phi_{sb} = -65^\circ$. Similar to the other asymmetries, the direct dependence on S_{LL} (D_{LL}) of the average values of P_{LN} with different values of B_{sb} and ϕ_{sb} for the case of muons and taus are shown in Figs. 3a (4a) and 5g 6g, respectively. It can be found out from these pictures that for the case of muons the value of $\langle P_{LN}\rangle$ fluctuates between the values -0.013 and$+0.033$ for the different values of new physics parameters while for taus, as final state leptons, the value of $\langle P_{LN}\rangle$ fluctuates between -0.04 and $+0.33$.

TABLE IX. Numerical values of $\langle P_{ij}\rangle$ in the Z' model without including LD effects.

			Using LCSR_{New}				
				$\lvert B_{sb}\rvert = 1.31$, $\phi_{sb} = -79^\circ$		$\lvert B_{sb}\rvert = 0.87$, $\phi_{sb} = -65^\circ$	
$\langle P_{ij}\rangle$	Decay Channel	Scenario-I	Scenario-II	$D_{LL} = 0$, $S_{LL} = -6.7$	$D_{LL} = -9.3$, $S_{LL} = 0$	$D_{LL} = 0$, $S_{LL} = 1.1$	$D_{LL} = -4.1$, $S_{LL} = 0$
$\langle P_{LL}\rangle$	$B \to K^*\mu^+\mu^-$	−0.910	−0.413	−0.701	−0.467	−0.841	−0.786
	$B \to K^*\tau^+\tau^-$	−0.456	−0.287	−0.334	−0.300	−0.465	−0.457
$\langle P_{LN}\rangle$	$B \to K^*\mu^+\mu^-$	−0.009	0.029	−0.033	−0.032	0.007	0.015
	$B \to K^*\tau^+\tau^-$	−0.017	0.300	−0.154	−0.304	0.095	0.159
$\langle P_{NL}\rangle$	$B \to K^*\mu^+\mu^-$	0.009	−0.029	0.033	0.032	−0.007	−0.015
	$B \to K^*\tau^+\tau^-$	0.017	−0.300	0.154	0.304	−0.095	−0.159
$\langle P_{LT}\rangle$	$B \to K^*\mu^+\mu^-$	−0.009	0.029	−0.033	0.032	0.007	0.015
	$B \to K^*\tau^+\tau^-$	−0.254	−0.388	−0.182	−0.364	−0.283	−0.317
$\langle P_{TL}\rangle$	$B \to K^*\mu^+\mu^-$	−0.04	−0.082	−0.028	−0.077	−0.047	−0.056
	$B \to K^*\tau^+\tau^-$	−0.0005	−0.230	0.004	−0.198	−0.025	−0.063
$\langle P_{NN}\rangle$	$B \to K^*\mu^+\mu^-$	−0.040	0.153	−0.099	0.130	0.015	0.050
	$B \to K^*\tau^+\tau^-$	−0.092	0.239	0.159	0.187	−0.046	0.020
$\langle P_{TT}\rangle$	$B \to K^*\mu^+\mu^-$	−0.036	0.144	0.091	0.122	0.022	0.052
	$B \to K^*\tau^+\tau^-$	0.037	−0.264	0.102	−0.218	−0.011	−0.070
$\langle P_{TN}\rangle$	$B \to K^*\mu^+\mu^-$	−0.030	0.161	−0.146	−0.179	0.029	0.084
	$B \to K^*\tau^+\tau^-$	0.0003	0.014	−0.005	0.015	0.003	0.007
$\langle P_{NT}\rangle$	$B \to K^*\mu^+\mu^-$	0.030	−0.161	0.146	0.179	−0.029	−0.084
	$B \to K^*\tau^+\tau^-$	−0.0003	−0.014	0.005	−0.015	−0.003	−0.007

TABLE X. Numerical values of $\langle P_{ij}\rangle$ in the Z' model with LD effects.

		Using $\mathbf{LCSR_{New}}$ ($\mathbf{Region\text{-}R_1}$)					
$\langle P_{ij}\rangle$	Decay Channel	Scenario I	Scenario II	$\lvert B_{sb}\rvert = 1.31, \phi_{sb} = -79^\circ$		$\lvert B_{sb}\rvert = 0.87, \phi_{sb} = -65^\circ$	
$\langle P_{LL}\rangle$	$B \to K^*\mu^+\mu^-$	−0.949	−0.944	−0.953	−0.944	−0.937	−0.941
	$B \to K^*\tau^+\tau^-$	…	…	…	…	…	…
$\langle P_{LN}\rangle$	$B \to K^*\mu^+\mu^-$	−0.017	0.0513	−0.054	0.055	0.007	0.023
	$B \to K^*\tau^+\tau^-$	…	…	…	…	…	…
$\langle P_{NL}\rangle$	$B \to K^*\mu^+\mu^-$	0.017	−0.0513	0.054	−0.055	−0.007	−0.023
	$B \to K^*\tau^+\tau^-$	…	…	…	…	…	…
$\langle P_{LT}\rangle$	$B \to K^*\mu^+\mu^-$	−0.086	−0.148	−0.063	−0.141	−0.092	−0.108
	$B \to K^*\tau^+\tau^-$	…	…	…	…	…	…
$\langle P_{TL}\rangle$	$B \to K^*\mu^+\mu^-$	−0.073	−0.148	−0.055	−0.137	−0.088	−0.103
	$B \to K^*\tau^+\tau^-$	…	…	…	…	…	…
$\langle P_{NN}\rangle$	$B \to K^*\mu^+\mu^-$	−0.096	0.272	−0.193	0.222	0.004	0.066
	$B \to K^*\tau^+\tau^-$	…	…	…	…	…	…
$\langle P_{TT}\rangle$	$B \to K^*\mu^+\mu^-$	−0.085	0.253	−0.176	0.207	0.021	0.072
	$B \to K^*\tau^+\tau^-$	…	…	…	…	…	…
$\langle P_{TN}\rangle$	$B \to K^*\mu^+\mu^-$	−0.058	0.302	−0.252	0.334	0.033	0.139
	$B \to K^*\tau^+\tau^-$	…	…	…	…	…	…
$\langle P_{NT}\rangle$	$B \to K^*\mu^+\mu^-$	0.058	−0.302	0.252	−0.334	−0.033	−0.139
	$B \to K^*\tau^+\tau^-$	…	…	…	…	…	…
		($\mathbf{Region\text{-}R_2}$)					
$\langle P_{LL}\rangle$	$B \to K^*\mu^+\mu^-$	−0.995	−0.995	−0.996	−0.996	−0.996	−0.996
	$B \to K^*\tau^+\tau^-$	−0.059	0.379	−0.140	0.304	−0.006	0.078
$\langle P_{LN}\rangle$	$B \to K^*\mu^+\mu^-$	−0.004	0.017	−0.019	0.018	0.009	0.012
	$B \to K^*\tau^+\tau^-$	−0.014	0.404	−0.185	0.410	0.104	0.197
$\langle P_{NL}\rangle$	$B \to K^*\mu^+\mu^-$	0.004	−0.017	0.019	−0.018	−0.009	−0.012
	$B \to K^*\tau^+\tau^-$	0.014	−0.404	0.185	−0.410	−0.104	−0.197
$\langle P_{LT}\rangle$	$B \to K^*\mu^+\mu^-$	−0.052	−0.057	−0.039	−0.057	−0.054	−0.057
	$B \to K^*\tau^+\tau^-$	−0.080	−0.137	−0.058	−0.126	−0.089	−0.102
$\langle P_{TL}\rangle$	$B \to K^*\mu^+\mu^-$	−0.015	−0.047	−0.012	−0.044	−0.023	−0.029
	$B \to K^*\tau^+\tau^-$	−0.006	−0.084	−0.003	−0.072	−0.013	−0.026
$\langle P_{NN}\rangle$	$B \to K^*\mu^+\mu^-$	−0.013	0.091	−0.049	0.081	0.009	0.035
	$B \to K^*\tau^+\tau^-$	−0.122	0.354	−0.205	0.270	−0.070	0.022
$\langle P_{TT}\rangle$	$B \to K^*\mu^+\mu^-$	−0.014	0.088	−0.048	0.077	0.008	0.032
	$B \to K^*\tau^+\tau^-$	−0.033	−0.446	0.049	−0.376	−0.090	−0.167
$\langle P_{NT}\rangle$	$B \to K^*\mu^+\mu^-$	−0.011	0.095	−0.086	0.103	0.041	0.065
	$B \to K^*\tau^+\tau^-$	0.0001	0.013	−0.005	0.014	0.003	0.006
$\langle P_{TN}\rangle$	$B \to K^*\mu^+\mu^-$	0.011	−0.095	0.086	−0.103	−0.041	−0.065
	$B \to K^*\tau^+\tau^-$	−0.0001	−0.013	0.005	−0.014	−0.003	−0.006

(vii) The s dependence of the polarization asymmetry P_{NN} is drawn in Fig. 1e for muons and in Fig. 2e for taus. These figures show that for muons (taus), P_{NN} is a decreasing (increasing) function of s. It is also clear from these graphs that in both cases, the Z' boson effects are constructive. For instance in the case of muons the maximum SM value of $P_{NN} = +0.35$ is enhanced up to, approximately, 41.67% on setting $B_{sb} = +1.31$, $D_{LL} = -9.3$, $S_{LL} = +1.1$, and $\phi_{sb} = -65^\circ$. On the other hand, for the case of taus with the same values of new physics parameters, the minimum SM value of P_{NN} at $4m_\tau^2$, which is near zero, is increased up to -0.45.

(viii) To check the dependency of $\langle P_{NN}\rangle$ on the choice of the form factors, one can see from Table VII that for the case of muons the value is of the order of 10^{-2} (i.e., below the optimal region), however, when we choose the PQCD form factors this value increase up

TABLE XI. Numerical values of $\langle P_{ij}\rangle$ in the Z' model with LD effects.

		Using $\mathbf{LCSR_{New}}$ (Region-$\mathbf{R_3}$)					
				$\lvert B_{sb}\rvert = 1.31$, $\phi_{sb} = -79^\circ$		$\lvert B_{sb}\rvert = 0.87$, $\phi_{sb} = -65^\circ$	
$\langle P_i\rangle$	Decay Channel	Scenario I	Scenario II	$D_{LL} = 0$, $S_{LL} = -6.7$	$D_{LL} = -9.3$, $S_{LL} = 0$	$D_{LL} = 0$, $S_{LL} = 1.1$	$D_{LL} = -4.1$, $S_{LL} = 0$
$\langle P_{LL}\rangle$	$B \to K^*\mu^+\mu^-$	−0.997	−0.997	−0.997	−0.997	−0.997	−0.997
	$B \to K^*\tau^+\tau^-$	−0.276	−0.068	−0.330	−0.093	−0.233	−0.189
$\langle P_{LN}\rangle$	$B \to K^*\mu^+\mu^-$	−0.002	0.010	−0.011	0.010	0.006	0.007
	$B \to K^*\tau^+\tau^-$	−0.037	0.270	−0.180	0.270	0.120	0.165
$\langle P_{NL}\rangle$	$B \to K^*\mu^+\mu^-$	0.002	−0.010	0.011	−0.010	−0.006	−0.007
	$B \to K^*\tau^+\tau^-$	0.037	−0.270	0.180	−0.270	−0.120	−0.165
$\langle P_{LT}\rangle$	$B \to K^*\mu^+\mu^-$	−0.037	−0.036	−0.028	−0.036	−0.038	−0.038
	$B \to K^*\tau^+\tau^-$	−0.311	−0.437	−0.212	−0.423	−0.350	−0.386
$\langle P_{TL}\rangle$	$B \to K^*\mu^+\mu^-$	−0.005	−0.027	−0.003	−0.025	−0.010	−0.014
	$B \to K^*\tau^+\tau^-$	−0.025	−0.305	−0.015	−0.270	−0.072	−0.121
$\langle P_{NN}\rangle$	$B \to K^*\mu^+\mu^-$	−0.003	0.019	−0.011	0.017	0.001	0.007
	$B \to K^*\tau^+\tau^-$	−0.032	0.299	−0.119	0.259	0.037	0.106
$\langle P_{TT}\rangle$	$B \to K^*\mu^+\mu^-$	−0.003	0.017	−0.010	0.015	0.001	0.006
	$B \to K^*\tau^+\tau^-$	−0.004	−0.308	0.081	−0.272	−0.071	−0.134
$\langle P_{NT}\rangle$	$B \to K^*\mu^+\mu^-$	−0.001	0.021	−0.018	0.023	0.009	0.015
	$B \to K^*\tau^+\tau^-$	−0.002	0.013	−0.006	0.014	0.004	0.007
$\langle P_{TN}\rangle$	$B \to K^*\mu^+\mu^-$	0.001	−0.021	0.018	−0.023	−0.009	−0.015
	$B \to K^*\tau^+\tau^-$	0.002	−0.013	0.006	−0.014	−0.004	−0.007

to order 10^{-1}. The graphs of the average value of P_{NN} vs S_{LL} (D_{LL}) are drawn in Figs. 3d 4d and 5d (6d) for muons and taus as final state leptons, respectively. As we have already noticed from Table VII, the value of $\langle P_{NN}\rangle$ is close to zero as can be seen in Figs. 3c and 3d. From these figures one sees that due to the presence of a Z' boson the average value either +ve or −ve, depends on the values of different new physics parameters. In addition, one can also note that the maximum value could be increased up to +0.15 or decreased up to −0.05. In the same way, Figs 5d and 6d (for the case of taus) show that the maximum value could be increased up to +0.25 or decreased up to −0.10 (see the blue and green shaded regions in these graphs).

(xi) In Figs. 1f and 2f, we have plotted P_{TT} as a function of s. It is noted that, as for P_{NN}, P_{TT} for $\mu^+\mu^-$ is also a decreasing function of s. This can also be seen for the case of muons where the new physics effects are quite prominent at low s; at larger s, these effects become mild and vanish for higher values of s. However, for the case of taus these effects are prominent throughout the available kinematic region and the minimum SM value of $P_{NN} = -0.2$ is shifted to −0.55 on setting $B_{sb} = +1.31$, $D_{LL} = -9.3$, $S_{LL} = +1.1$, and $\phi_{sb} = -65^\circ$. Similarly, $\langle P_{TT}\rangle$ is plotted against S_{LL} (D_{LL}) in Figs. 3f, 4f and 5f, 6f for muons and taus, respectively, and exhibits the same kind of behavior as $\langle P_{NN}\rangle$, but for the case of taus the sign of $\langle P_{TT}\rangle$ is opposite to $\langle P_{NN}\rangle$.

It is also necessary to mention here that the numerical values of all nine double lepton polarization asymmetries in the SM and in the Z' model are displayed in Tables VII to XI where one can also see the variations of these values on different values of new physics parameters, on different form factors, and on the inclusion/exclusion of long distance effects.

In the last set of results from Figs. 7, 8, 9, and 10, we present the correlation between the branching ratio of $B \to K^*\mu^+\mu^-$ and various double lepton polarization asymmetries. It is clear from these graphs that in some parameter space of extra gauge boson model, even if the branching ratio is not changed significantly from its SM value, various polarization asymmetries can show substantial variation in their values. This feature is due to the fact that the asymmetries dependence on Wilson Coefficients and at the branching ratio is different and provides independent information about new physics.

Finally, since the subject is somewhat topical, to get more concrete we supplement our numerical results with some qualitative estimates of the number of decay events needed to experimentally probe their calculated effects, and check them with the expected reach, for example, at the CERN experiment LHCb. In this regard, at the $n\sigma$ level, the minimum number of required $B\bar{B}$ pairs is given by the following formula [89]

$$N = \frac{n^2}{\mathcal{B}s_1 s_2\langle O\rangle}, \tag{47}$$

where $\mathcal{B}$ is the branching ratio of the decay channel under consideration, i.e., $B \to K^*\ell^+\ell^-$ and s_1, s_2 are the reconstruction efficiencies of the final leptons. The

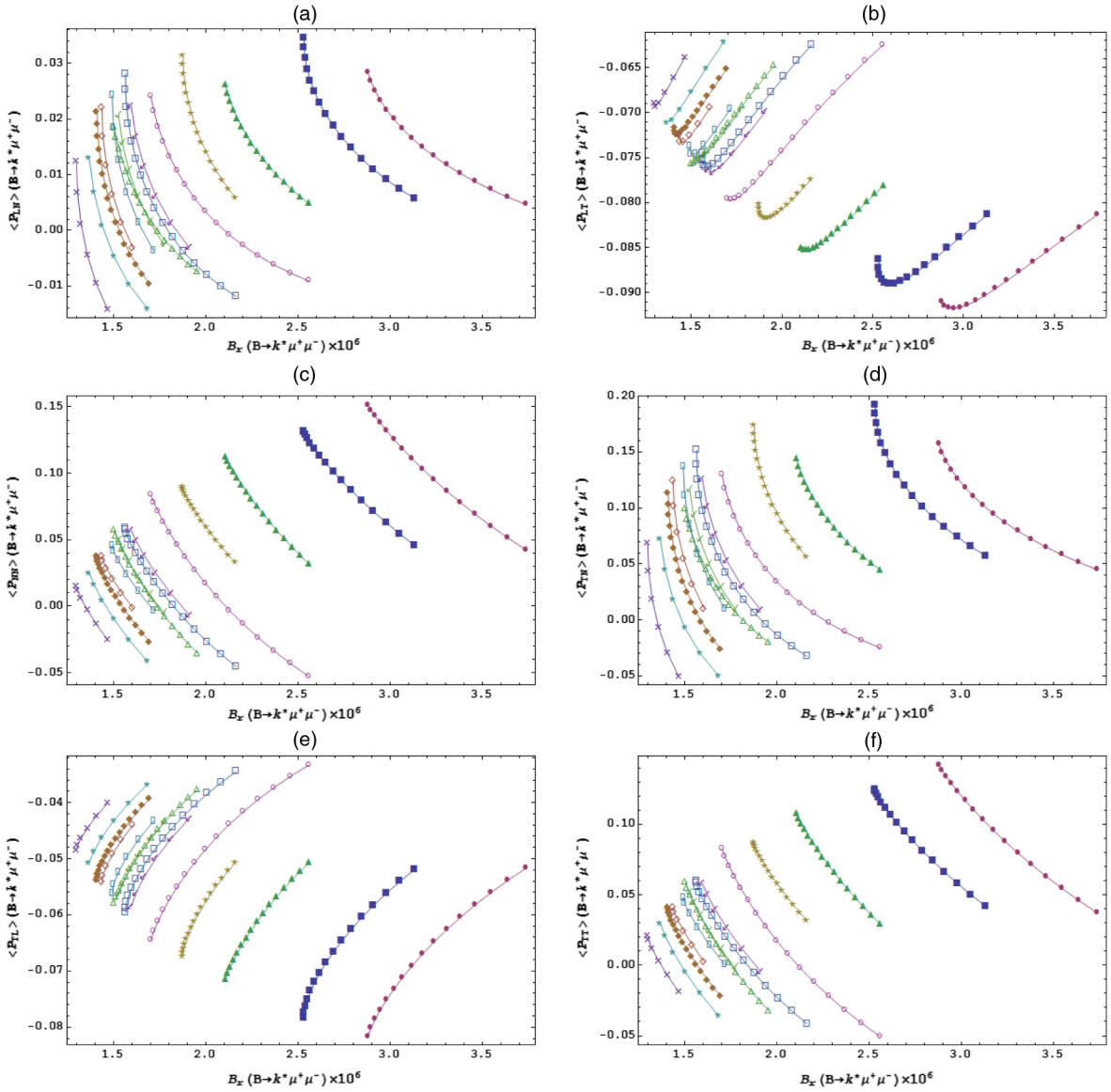

FIG. 7 (color online). Plots of double lepton polarization asymmetries vs branching ratio of $B \to K^* l^+ l^-$ when we fix the values of different parameters of the Z' model and vary the value of S_{LL} throughout its allowed region in S_1 and S_2, for $\mu^+\mu^-$ as final state leptons.

efficiency of τ lepton is taken to be 0.5 as the values of τ detection efficiencies and its polarization asymmetries have large errors [90,91]. By using the above formula to observe the various polarization asymmetries at 3σ level, the following number of events are needed:

(i) For $B \to K^*\mu^+\mu^-$

$$N \sim \begin{cases} 10^6 & \text{for } \langle P_{LL}\rangle, \\ 10^9 & \text{for } \langle P_{LT}\rangle, \langle P_{TL}\rangle \\ 10^{10} & \text{for } \langle P_{TT}\rangle, \\ 10^{11} & \text{for } \langle P_{NN}\rangle, \langle P_{TN}\rangle, \langle P_{NT}\rangle \\ 10^{12} & \text{for } \langle P_{LN}\rangle, \langle P_{NL}\rangle. \end{cases}$$

(ii) For $B \to K^*\tau^+\tau^-$

$$N \sim \begin{cases} 10^9 & \text{for } \langle P_{LL}\rangle, \langle P_{LT}\rangle \\ 10^{10} & \text{for } \langle P_{LN}\rangle, \langle P_{NL}\rangle, \langle P_{NN}\rangle, \langle P_{TL}\rangle, \\ 10^{11} & \text{for } \langle P_{TT}\rangle, \\ 10^{13} & \text{for } \langle P_{TN}\rangle, \langle P_{NT}\rangle. \end{cases}$$

On the other hand, the number of $B\bar{B}$ produced at LHC experiments such as LHCb, CMS, and ATLAS are around 10^{12} per year, whereas, at Super-LHC this number is raised up to 10^{13}. These statistics shows that there is a good chance that all the double lepton polarization asymmetries of $B \to K^* l^+ l^-$ will be measured at LHC except

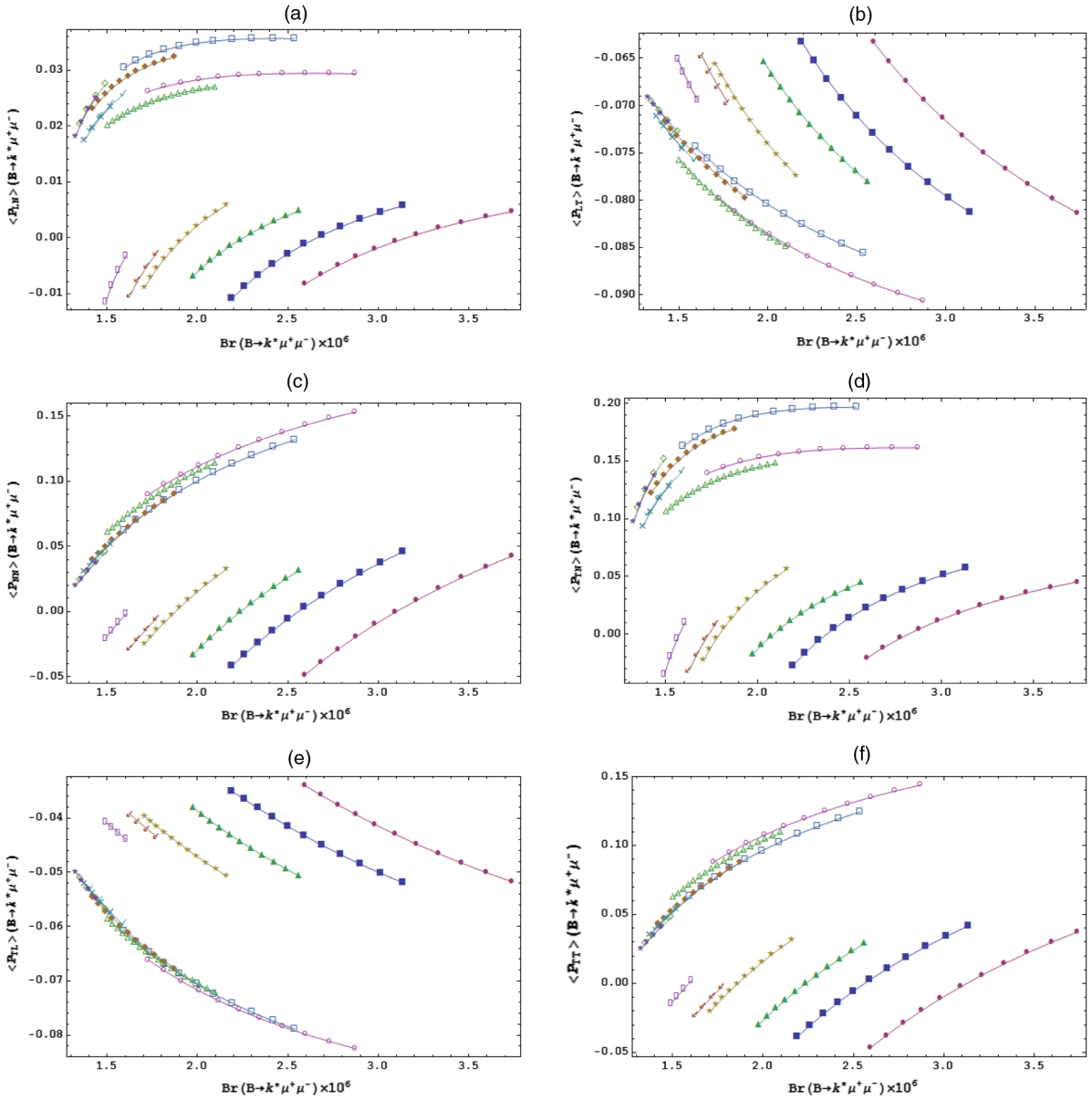

FIG. 8 (color online). Plots of double lepton polarization asymmetries vs branching ratio of $B \to K^* l^+ l^-$ when we fix the values of different parameters of the Z' model and vary the value of D_{LL} throughout its allowed region in S_1 and S_2, for $\mu^+\mu^-$ as final state leptons.

$\langle P_{TN} \rangle = \langle -P_{NT} \rangle$ which could only be seen at SLHC. However, in our case the extra gauge boson Z' effects are constructive for some tiny polarization asymmetries and bring their values to the observable range of LHC. In addition, it is important to note that even if to measure the lepton polarization of muons, the required number of $B\bar{B}$ pairs are comparatively less than the tau case, muons lepton polarizations are only possible when muons are at rest, and at present it seems hard to achieve this at the current colliders. On the other hand, the polarizations of τ can be studied through its decay products, therefore, one faces the uncertainty in the reconstruction efficiencies. However, the measurement of τ polarization is comparatively easier than the case of muon. Finally, if these technical issues will be resolved then these asymmetries are good observables to find out the impact of a Z' boson.

V. SUMMARY AND CONCLUSION

In this paper, we have studied the effects of an extra gauge boson (i.e., the Z' model) on the double lepton polarization asymmetries of $B \to K^* l^+ l^-$ decay where $l = \mu$ or τ. To achieve this target, first we have drawn these asymmetries as a function of s by choosing different values of Z' parameters. Similarly, to see the sensitivity of the average values of double polarization asymmetries on Z' boson, we have plotted $\langle P_{ij} \rangle$ against two independent parameters of the Z' model, namely, S_{LL} and D_{LL} which

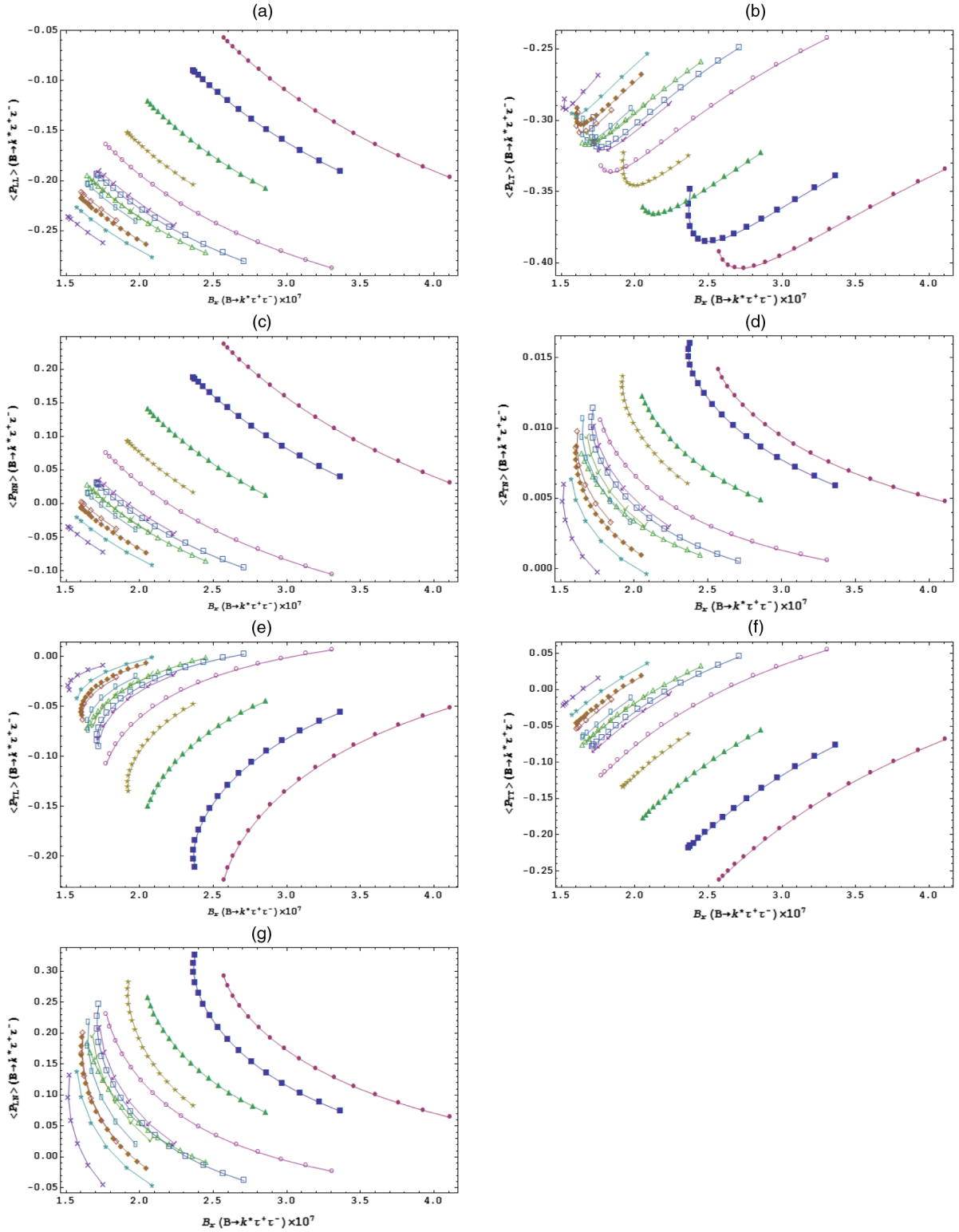

FIG. 9 (color online). Legends are the same as in Fig. 7 but for double lepton polarization asymmetries vs branching ratio of $B \to K^*\tau^+\tau^-$.

represent the combination of left- and right-handed couplings of Z' boson with the leptons. For the numerical values of Z' parameters, we have taken the values of these parameters from the allowed regions which are constrained by different inclusive and exclusive B decays [14,63]. The form factors give us some insight about the nonperturbative regime, which is not fully understood yet, and are the main source of uncertainty in the calculation. In the literature,

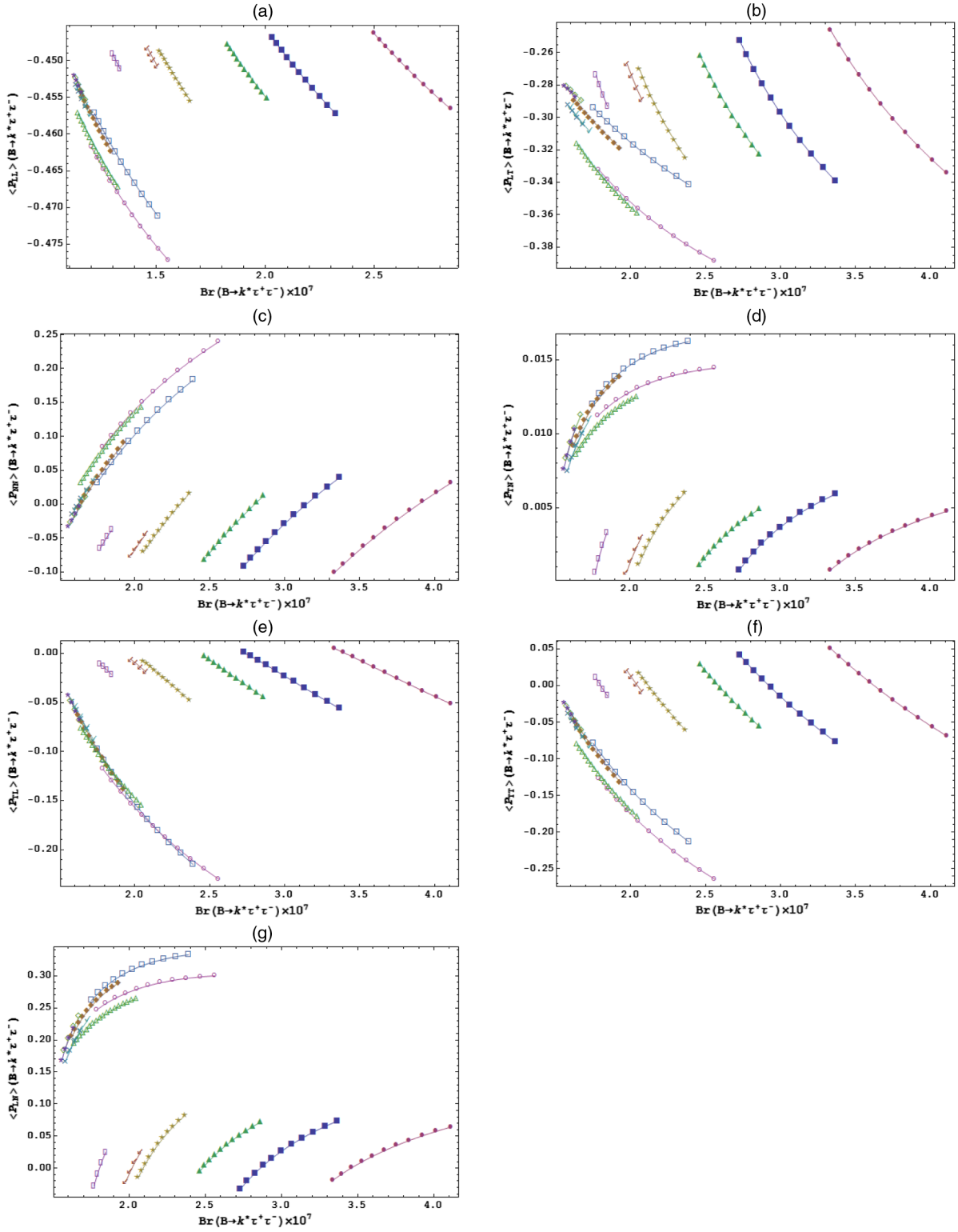

FIG. 10 (color online). Legends are the same as in Fig. 8 but for double lepton polarization asymmetries vs branching ratio of $B \to K^* \tau^+ \tau^-$.

these form factors are calculated through various non-perturbative methods which are some what independent of each other. In this context, we have chosen four different types of form factors and calculated the average values of various polarization asymmetries and listed their numerical values in different tables by setting the different values of Z' parameters with and without including resonance effects. It is found that the values of some asymmetries are quite

sensitive to the choice of the form factors. However, to investigate the Z' boson effects in the lepton polarization asymmetries, we plot them against the square of the momentum transfer s by using the recently calculated LCSR form factors, whereas their average numerical values are calculated using two different form factors, namely, LCSR and PQCD. It is found that the various polarization asymmetries can significantly deviate from their SM values. Apart from the magnitude of these asymmetries which can be reduced or enhanced due to the influence of Z' boson, the sign of some of these asymmetries can also be flipped. In addition, we have found that the values of $\langle P_{TN}\rangle$, $\langle P_{LN}\rangle$ which are small in SM get enlarged in the Z' model and must be visible at the LHC; therefore, measurement of these asymmetries will provide a clear signature of new physics. Finally, we have drawn these asymmetries as a function of the branching ratio, whereupon, one can assure that these asymmetries can provide independent information about new physics.

To sum up, the measurement of double lepton polarization asymmetries at LHC would play a crucial role in investigating the existence of the Z' gauge boson as well as help out to constrain the values of the coupling of Z' boson with SM particles. As we have shown, these asymmetries are also sensitive to nonperturbative physics so precise measurements of these asymmetry may also give some clues to understanding the long distance regime of QCD.

ACKNOWLEDGMENTS

The author would like to thank referee for help in improving the presentation of the manuscript.

[1] T. Asltonen *et al.* (CDF Collaboration); V. M. Abazov *et al.* (DØ Collaboration), CDF Report No. CDF/PHYS/BOTTOM/CDFR/9878, 2009; (DØ Collaboration) Report No. 5928-CONF, 2009 (unpublished).
[2] B. Aubert *et al.* (*BABAR* Collaboration), Phys. Rev. Lett. **91**, 171802 (2003).
[3] K. F. Chen *et al.* (Belle Collaboration), Phys. Rev. Lett. **91**, 201801 (2003).
[4] B. Aubert *et al.* (*BABAR* Collaboration), Phys. Rev. D **79**, 031102 (2009).
[5] V. M. Abazov *et al.* arXiv:1005.2757.
[6] N. Arkani-Hamed, A. G. Cohen, E. Katz, and A. E. Nelson, J. High Energy Phys. 07 (**2002**) 034.
[7] S. Chang and H. J. He, Phys. Lett. B **586**, 95 (2004).
[8] T. Appelquist, H. C. Cheng, and B. A. Doberscu, Phys. Rev. D **64**, 035002 (2001).
[9] C. Csaki, Mod. Phys. Lett. A **11**, 599 (1996).
[10] P. Langacker and Plümacher, Phys. Rev. D **62**, 013006 (2000).
[11] P. Frampton, P. Hung, and M. Sher, Phys. Rep. **330**, 263 (2000).
[12] V. Barger, L. Everett, J. Jiang, P. Langacker, T. Liu, and C. Wagner, Phys. Rev. D **80**, 055008 (2009); J. High Energy Phys. 12 (**2009**) 048.
[13] V. Barger, C. W. Chiang, P. Langacker, and H. S. Lee, Phys. Lett. B **598**, 218 (2004); also see the first ref in Ref. 48.
[14] Q. Chang, X. Q. Li, and Y. D. Yang, J. High Energy Phys. 02 (**2010**) 082.
[15] W. S. Hou. Nagashima, and A. Soddu, Phys. Rev. D **72**, 115007 (2005).
[16] W. S. Hou. Nagashima, and A. Soddu, Phys. Rev. D **76**, 016004 (2007).
[17] A. Soni, A. K. Alok, A. Giri, R. Mohanta, and S. Nandi, Phys. Lett. B **683**, 302 (2010).
[18] A. Soni, A. K. Alok, A. Giri, R. Mohanta, and S. Nandi, Phys. Lett. **82B**, 033009 (2010).
[19] A. J. Buras, B. Duling, T. Feldmann, T. Heidsieck, C. Promberger, and S. Recksiegel, J. High Energy Phys. 09 (**2010**) 106.
[20] W. S. Hou and C. Y. Ma, Phys. Rev. D **82**, 036002 (2010).
[21] T. Moroi, Phys. Lett. B **493**, 366 (2000).
[22] D. Chang, A. Masiero, and H. Murayama, Phys. Rev. D **67**, 075013 (2003).
[23] R. Harnik, D. T. Larson, H. Murayama, and A. Pierce, Phys. Rev. D **69**, 094024 (2004).
[24] M. Ciuchini, E. Franco, A. Masiero, and L. Silvestrini, Phys. Rev. D **67**, 075016 (2003).
[25] J. Foster, K.-i. Okumura, and L. Roszkowski, J. High Energy Phys. 08 (**2005**) 094.
[26] M. Blanke, A. J. Buras, B. Duling, S. Gori, and A. Weiler, J. High Energy Phys. 03 (**2009**) 001.
[27] M. Blanke, A. J. Buras, B. Duling, K. Gemmler, and S. Gori, J. High Energy Phys. 03 (**2009**) 108.
[28] M. Blanke, , A. J. Buras, A. Poschenrieder, C. Tarantino, S. Uhlig, and A. Weiler, J. High Energy Phys. 12 (**2006**) 003.
[29] V. Barger, L. L. Everett, J. Jiang, P. Langacker, T. Liu, and C. E. M. Wagner, J. High Energy Phys. 12 (**2009**) 048.
[30] T. M. Aliev, V. Bashiry, and M. Savci, Eur. Phys. J. C **35**, 197 (2004).
[31] T. M. Aliev, V. Bashiry, and M. Savci, Phys. Rev. D **72**, 034031 (2005).
[32] T. M. Aliev, V. Bashiry, and M. Savci, J. High Energy Phys. 05 (**2004**) 037.
[33] T. M. Aliev, V. Bashiry, and M. Savci, Phys. Rev. D **73**, 034013 (2006).
[34] T. M. Aliev, V. Bashiry, and M. Savci, Eur. Phys. J. C **40**, 505 (2005).
[35] Chuan-Hung Chen and C. Q. Geng, Phys. Lett. B **516**, 327 (2001).
[36] V. Bashiry, Chin. Phys. Lett. **22**, 2201 (2005).
[37] W. S. Hou, R. S. Willey, and A. Soni, Phys. Rev. Lett. **58**, 1608 (1987); Phys. Rev. Lett. **60**, 2337(E) (1988).

[38] T. Hattori, T. Hasuike, and S. Wakaizumi, Phys. Rev. D **60**, 113008 (1999).
[39] Y. Dincer, Phys. Lett. B **505**, 89 (2001) and references therein.
[40] C. S. Huang, W. J. Huo, and Y. L. Wu, Phys. Rev. D **64**, 016009 (2001).
[41] A. K. Alok, *et al.*, J. High Energy Phys. 02 (**2010**) 053.
[42] A. Ali, T. Mannel, and T. Morosumi, Phys. Lett. B **273**, 505 (1991).
[43] C. W. Chiang, R. H. Li, and C. D. Lu, Chin. Phys. C **36**, 14 (2012).
[44] P. Colangelo, F. De Fazio, R. Feerandes, and T. N. Pham, Phys. Rev. D **74**, 115006 (2006).
[45] A. Ahmed, I. Ahmed, M. A. Paracha, and A. Rehman, Phys. Rev. D **84**, 033010 (2011).
[46] T. M. Aliev, A. Ozpineci, and M. Savci, Phys. Lett. B **511**, 49 (2001).
[47] Q. Chang and Yin-Hao GaoarXiv:1101.1272v1; Y. Li and J. Hua, Eur. Phys. J. C **71**, 1775 (2011).
[48] A. Ali, P. Ball, L. T. Handoko, and G. Hiller, Phys. Rev. D **61**, 074024 (2000).
[49] G. Buchalla, A. J. Buras, and M. E. Lautenbacher, Rev. Mod. Phys. **68**, 1125 (1996).
[50] A J. Buras and M. Munz, Phys. Rev. D **52**, 186 (1995).
[51] A. J. Buras, M. Misiak, M. Munz, and S. Pokorski, Nucl. Phys. **B424**, 374 (1994).
[52] F. Kruger and L. M. Sehgal, Phys. Lett. **380**, 199 (1996).
[53] B. Grinstein, M. J. Savag, and M. B. Wise, Nucl. Phys. **B319**, 271 (1989).
[54] G. Cella, G. Ricciardi, and A. Vicere, Phys. Lett. B **258**, 212 (1991).
[55] C. Bobeth, M. Misiak, and J. Urban, Nucl. Phys. **B574**, 291 (2000).
[56] H. H. Asatrian, H. M. Asatrian, C. Grueb, and M. Walker, Phys. Lett. B **507**, 162 (2001).
[57] M. Misiak, Nucl. Phys. **B393**, 23 (1993); Nucl. Phys. **B439**, 461(E) (1995).
[58] T. Huber, T. Hurth, and E. Lunghi, arXiv:0807.1940.
[59] W. Altmannshofer, P. Ball, A. Bharucha, A. J. Buras, D. M. Straub, and M. Wick, J. High Energy Phys. 01 (**2009**) 019.
[60] A. J. Buras and M. Munz, Phys. Rev. D **52**, 186 (1995).
[61] W. Altmannshofer, P. Ball, A. Bharucha, A. J. Buras, D. M. Straub, and M. Wick, J. High Energy Phys. 01 (**2009**) 019.
[62] Cheng-Wei. Chiang, Run-Hui Li, and Cai-Dian Lu, Chin. Phys. C **36**, 14 (2012).
[63] Q. Chang, X. Q. Li, and Y. D. Yang, J. High Energy Phys. 05 (**2009**) 056; Q. Chang, X. Q. Li, and Y. D. Yang, J. High Energy Phys. 04 (**2010**) 052.
[64] K. Cheung, C.-W. Chiang, N. G. Deshpande, and J. Jiang, Phys. Lett. B **652**, 285 (2007); C. H. Chen and H. Hatanaka, Phys. Rev. D **73**, 075003 (2006); C. W. Chiang, N. G. Deshpande, and J. Jiang, J. High Energy Phys. 08 (**2006**) 075.
[65] V. Berger, C.-W. Chiang, P. Langacker, and H.-S. Lee, Phys. Lett. B **580**, 186 (2004); V. Berger, L. Everett, J. Jiang, P. Langacker, T. Liu, and C. Wagner, Phys. Rev. D **80**, 055008 (2009); R. Mohanta and A. K. Giri, Phys. Rev. D **79**, 057902 (2009); J. Hua, C. S. Kim, and Y. Li, Eur. Phys. J. C **69**, 139 (2010).
[66] A. K. Alok, A. Datta, A. Dighe, M. Duraisamy, D. Ghosh, and D. London, J. High Energy Phys. 11 (**2011**) 121.
[67] A. Ali, T. Mannel, and T. Morozumi, Phys. Lett. B **273**, 505 (1991).
[68] A. J. Buras and M. Munz, Phys. Rev. D **52**, 186 (1995).
[69] M. Misiak, Nucl. Phys. **B393**, 23 (1993); Nucl. Phys. **B439**, 461(E) (1995).
[70] F. Kruger and E. Lunghi, Phys. Rev. D **63**, 014013 (2000).
[71] A. Ali, E. Lunghi, C. Greub, and G. Hiller, Phys. Rev. D **66**, 034002 (2002).
[72] A. Ghinculov, T. Hurth, G. Isidori, and Y. P. Yao, Eur. Phys. J. C **33**, s288 (2004).
[73] D. Melikhov and B. Stech, Phys. Rev. D **62**, 014006 (2000).
[74] C. Chen and C. Q. Geng, Nucl. Phys. **B636**, 338 (2002).
[75] P. Ball and R. Zwicky, Phys. Rev. D **71**, 014029 (2005).
[76] R. R. Horgan, Z. Liu, S. Meinel, and M. Wingate, arXiv:1310.3887.
[77] A. Ali, G. Kramer, and G.-h. Zhu, Eur. Phys. J. C **47**, 625 (2006).
[78] A. K. Alok, A. Dighe, D. Ghosh, D. London, J. Matias, M. Nagashima, and A. Szynkman, J. High Energy Phys. 02 (**2010**) 053.
[79] F. Kruger and L. M. Sehgal, Phys. Lett. B **380**, 199 (1996).
[80] S. Fukae, C. S. Kim, and T. Yoshikawa, Phys. Rev. D **61**, 074015 (2000).
[81] W. Bensalem, D. London, N. Sinha, and R. Sinha, Phys. Rev. D **67**, 034007 (2003).
[82] S. Fukae, C. S. Kim, and T. Yoshikawa, Phys. Rev. D **61**, 074015 (2000).
[83] S. R. Choudhury, N. Gaur, A. S. Cornell, and G. C. Joshi, Phys. Rev. D **68**, 054016 (2003).
[84] K. Nakamura *et al.* (Particle Data Group), J. Phys. G **37**, 075021 (2010).
[85] A. Ali, P. Ball, L. T. Handoko, and G. Hiller, Phys. Rev. D **61**, 074024 (2000); arXiv:hep-ph/9910221.
[86] M. Bona *et al.*, (UTfit Collaboration), PMC Phys. A **3**, 6 (2009); M. Bona *et al.*, arXiv:0906.0953.
[87] Q. Chang and Y.-H. Gao, Nucl. Phys. **B845**, 179 (2011).
[88] C. Q. Geng, C. W. Hwang, and C. C. Liu, Phys. Rev. D **65**, 094037 (2002).
[89] T. M. Aliev and M. Savci, Phys. Lett. B **718**, 566 (2012).
[90] G. Abbidendi *et al.* (OPAL Collaboration), Phys. Lett. B **492**, 23 (2000).
[91] A. Rouge, Z. Phys. C **48**, 75 (1990); A. Rouge in Proceedings of the Workshop on τ Lepton Physics, Orsay, France 1990 (to be published).